Gastroenterology 2019;156:1788–1804

BASIC AND TRANSLATIONAL—LIVER

Estrogen Activation of G-Protein–Coupled Estrogen Receptor 1 Regulates Phosphoinositide 3-Kinase and mTOR Signaling to Promote Liver Growth in Zebrafish and Proliferation of Human Hepatocytes

Saireudee Chaturantabut,[1] Arkadi Shwartz,[1] Kimberley J. Evason,[2] Andrew G. Cox,[1,3] Kyle Labella,[1] Arnout G. Schepers,[4] Song Yang,[5] Mariana Acuña,[6] Yariv Houvras,[7] Liliana Mancio-Silva,[4] Shannon Romano,[8] Daniel A. Gorelick,[8] David E. Cohen,[6] Leonard I. Zon,[5,9,10,11] Sangeeta N. Bhatia,[4,12,13] Trista E. North,[5,10] and Wolfram Goessling[1,10,11,12,13,14]

[1]Genetics Division, Brigham and Women's Hospital, Harvard Medical School, Boston, Massachusetts; [2]Department of Pathology, University of Utah, Salt Lake City, Utah; [3]Peter MacCallum Cancer Centre, Melbourne, Victoria, Australia; [4]Koch Institute for Integrative Cancer Research, Massachusetts Institute of Technology, Cambridge, Massachusetts; [5]Stem Cell Program, Division of Hematology/Oncology, Boston Children's Hospital, Boston, Massachusetts; [6]Division of Gastroenterology and Hepatology, Weill Cornell Medical College, New York, New York; [7]Departments of Surgery and Medicine, Weill Cornell Medical College, New York, New York; [8]Department of Pharmacology and Toxicology, University of Alabama at Birmingham, Birmingham, Alabama; [9]Howard Hughes Medical Institute, Chevy Chase, Maryland; [10]Harvard Stem Cell Institute, Cambridge, Massachusetts; [11]Dana-Farber Cancer Institute, Boston, Massachusetts; [12]Harvard–MIT Division of Health Sciences and Technology, Cambridge, Massachusetts; [13]Broad Institute of MIT and Harvard, Cambridge, Massachusetts; and [14]Divison of Gastroenterology, Massachusetts General Hospital, Boston, Massachusetts

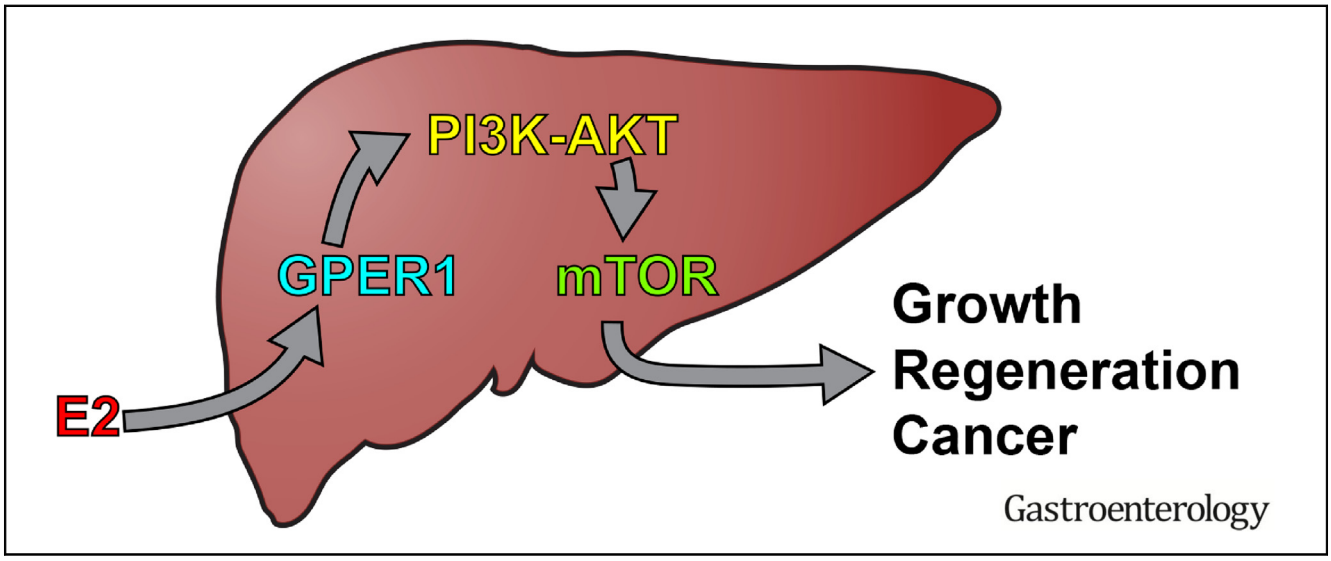

BACKGROUND & AIMS: Patients with cirrhosis are at high risk for hepatocellular carcinoma (HCC) and often have increased serum levels of estrogen. It is not clear how estrogen promotes hepatic growth. We investigated the effects of estrogen on hepatocyte proliferation during zebrafish development, liver regeneration, and carcinogenesis. We also studied human hepatocytes and liver tissues. **METHODS:** Zebrafish were exposed to selective modifiers of estrogen signaling at larval and adult stages. Liver growth was assessed by gene expression, fluorescent imaging, and histologic analyses. We monitored liver regeneration after hepatocyte ablation and HCC development after administration of chemical carcinogens (dimethylbenzanthrazene). Proliferation of human hepatocytes was measured in a coculture system. We measured levels of G-protein–coupled estrogen receptor (GPER1) in HCC and nontumor liver tissues from 68 patients by immunohistochemistry. **RESULTS:** Exposure to 17β-estradiol (E2) increased proliferation of hepatocytes and liver volume and mass in larval and adult zebrafish. Chemical genetic and epistasis experiments showed that GPER1 mediates the effects of E2 via the phosphoinositide 3-kinase–protein kinase B–mechanistic target of rapamycin pathway: *gper1*-knockout and *mtor*-knockout zebrafish did not increase liver growth in response to E2. HCC samples from patients had increased levels of GPER1 compared

with nontumor tissue samples; estrogen promoted proliferation of human primary hepatocytes. Estrogen accelerated hepatocarcinogenesis specifically in male zebrafish. Chemical inhibition or genetic loss of GPER1 significantly reduced tumor development in the zebrafish. **CONCLUSIONS:** In an analysis of zebrafish and human liver cells and tissues, we found GPER1 to be a hepatic estrogen sensor that regulates liver growth during development, regeneration, and tumorigenesis. Inhibitors of GPER1 might be developed for liver cancer prevention or treatment. **TRANSCRIPT PROFILING:** The accession number in the Gene Expression Omnibus is GSE92544.

Keywords: Sex Hormone; Signal Transduction; Transcription Regulation; Hepatocarcinogenesis.

WHAT YOU NEED TO KNOW

BACKGROUND

Patients with cirrhosis are at high risk for hepatocellular carcinoma (HCC) and often have increased serum levels of estrogen. It is not clear how estrogen promotes hepatic growth.

FINDINGS

Exposure to 17 beta-estradiol (E2) increased proliferation of hepatocytes and liver volume and mass in larval and adult zebrafish. GPER1 is a hepatic estrogen sensor that regulates liver growth during development, regeneration, and tumorigenesis. HCC samples from patients had increased levels of GPER1, compared with non-tumor tissues.

LIMITATIONS

This study was performed in an animal model of HCC.

IMPLICATIONS FOR PATIENTS

Inhibitors of GPER1 might be developed for liver cancer prevention or treatment.

Hepatocellular carcinoma (HCC) is the second most common cause of cancer mortality worldwide, and it is the fastest-growing cause of cancer deaths in the United States.[1] Clinically relevant biomarkers and therapies to detect and prevent HCC do not exist. Chronic liver disease and liver cancer are much more common in males,[2] and men with cirrhosis and HCC have elevated serum estrogen levels.[3,4] Furthermore, patients having surgical liver resection display elevated serum levels of estrogen, suggesting the importance of estrogenic regulation during liver regeneration.[5] The mechanisms by which the liver senses and responds to estrogen to affect liver growth and cancer formation remain undetermined.

17β-estradiol (E2) is the most abundant biologically active form of estrogen. Canonical estrogen signaling is mediated through nuclear hormone estrogen receptors 1 (ESR1/ERα) and 2 (ESR2/ERβ), resulting in transcriptional target gene activation. In addition, E2 can exert noncanonical activity through the G-protein–coupled estrogen receptor 1 (GPER1, also known as GPR30). Although the roles of ESR1 and ESR2 have been widely studied in the context of reproductive biology and cancer,[6] the functional consequences of GPER1 signaling are less well understood. Originally discovered in breast cancer cells,[7] GPER1 regulates the proliferation and relaxation of vascular smooth muscle.[8] Several secondary messenger signals have been identified in different cellular contexts, including extracellular signal-regulated kinase,[7] phosphoinositide 3-kinase (PI3K),[9] and $Ca2^{+}$ release.[10] *GPER1* expression in hepatocytes and its potential role in hepatocyte proliferation and organ growth during development, liver regeneration, or cancer progression have not been previously characterized.

Here, we identify the essential function of E2 and GPER1 in the regulation of liver growth. E2 induces cell cycle progression and increases hepatocyte proliferation and liver size in larval zebrafish. Surprisingly, these effects are not mediated through classic nuclear hormone estrogen receptors but via GPER1 and downstream activation of PI3K–mechanistic target of rapamycin (mTOR) signaling. GPER1 promotes sex-specific adult liver growth and, together with mTOR, is required for optimal liver regrowth after injury. In addition, GPER1 directly modulates liver cancer formation: *gper1*$^{-/-}$ fish develop significantly fewer and smaller liver tumors than wild-type siblings. The role of GPER1 is conserved in human liver, because liver cancer tissue expresses increased GPER1, and primary human hepatocytes activate protein kinase B (AKT)/mTOR and proliferate in response to E2. Chemical inhibition of GPER1 in vivo significantly diminishes E2-induced tumor progression after chemical carcinogenesis, particularly in males. We propose that GPER1 senses E2 to regulate PI3K/mTOR activity and cellular proliferation during hepatic development and repair and, as such, is an important therapeutic target for liver cancer prevention and treatment.

Materials and Methods

Zebrafish Husbandry

Zebrafish were maintained according to Institutional Animal Care and Use Committee guidelines at Harvard Medical School.

Chemical Exposures

Zebrafish larvae were exposed to chemical modifiers, dissolved in 0.1% (volume/volume) dimethyl sulfoxide (DMSO) for 5 hours from 110 to 115 hours postfertilization (hpf), and

Abbreviations used in this paper: **Akt, protein kinase B; DMBA, dimethylbenzanthracene; DMSO, dimethyl sulfoxide; ERE, estrogen response element; E2, 17β-estradiol; ESR, estrogen receptor; Erk, extracellular signal–regulated kinase; GFP, green fluorescent protein; GPER1, G protein-coupled estrogen receptor 1; HCC, hepatocellular carcinoma; hpf, hours post fertilization; IHC, immunohistochemistry; ISH, in situ hybridization; mTOR, mechanistic target of rapamycin; mTORC1, mTOR complex 1; mRNA, messenger RNA; Mtz, metronidazole; p-, phosphorylated; PCNA, proliferating cell nuclear antigen; PI3K, phosphoinositide 3-kinase; qRT-PCR, quantitative reverse transcription polymerase chain reaction; TALEN, transcription activator-like effector nuclease; TUNEL, terminal deoxynucleotidyl transferase deoxyuridine nick-end labeling; WT, wild type.**

Most current article

0016-5085/$36.00
https://doi.org/10.1053/j.gastro.2019.01.010

analyzed at 120 hpf (unless otherwise specified).[11] Adults were treated for 5–7 hours per exposure. Chemicals are listed in Supplementary Table 1.

Morpholino Injection

Morpholino oligonucleotides designed against *esr1, esr2a, esr2b*,[11] *gper1*, and *mtor* (Gene Tools, Philomath, OR)

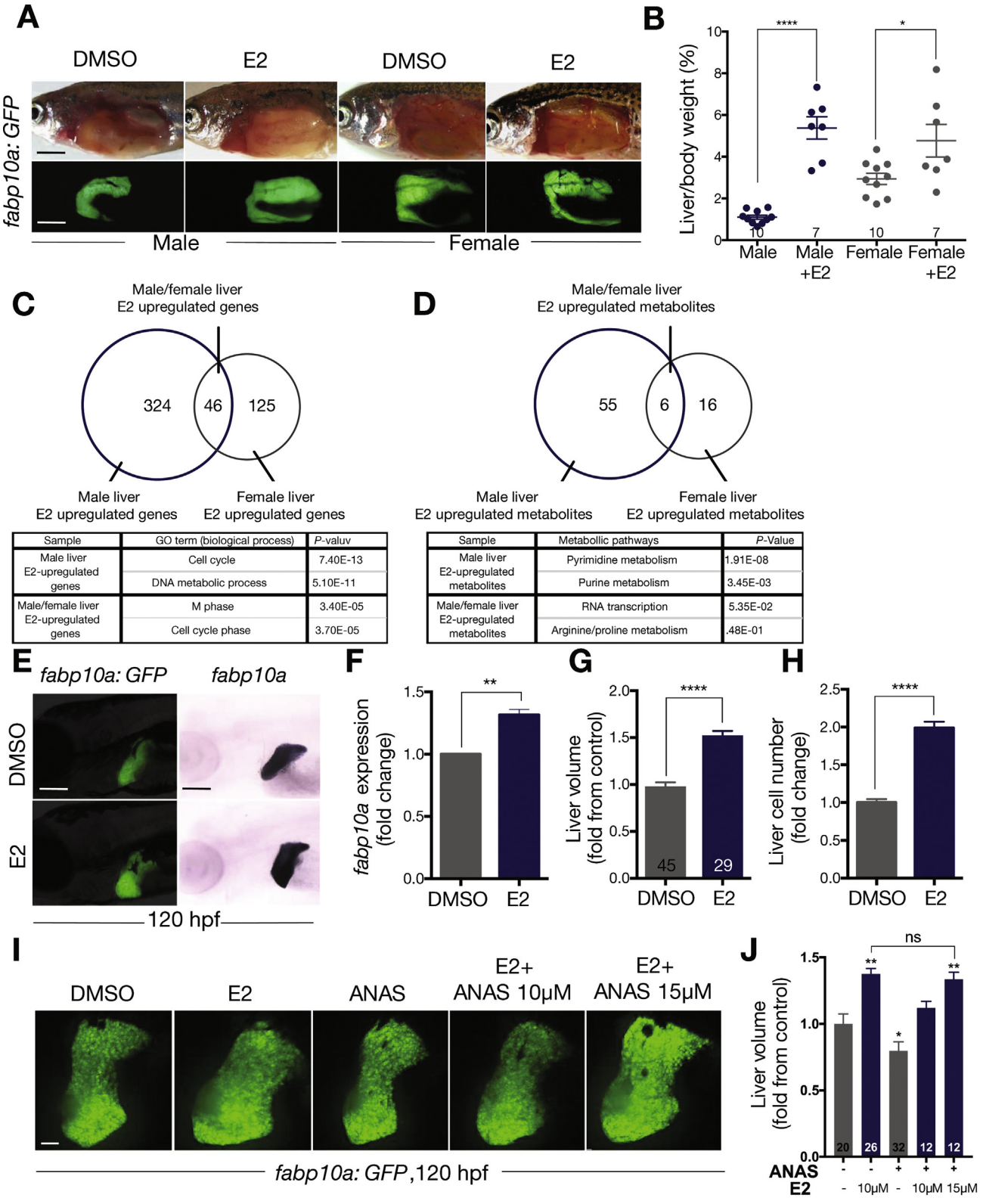

Sample	GO term (biological process)	*P*-valuv
Male liver E2-upregulated genes	Cell cycle	7.40E-13
	DNA metabolic process	5.10E-11
Male/female liver E2-upregulated genes	M phase	3.40E-05
	Cell cycle phase	3.70E-05

Sample	Metabolic pathways	*P*-Value
Male liver E2-upregulated metabolites	Pyrimidine metabolism	1.91E-08
	Purine metabolism	3.45E-03
Male/female liver E2-upregulated metabolites	RNA transcription	5.35E-02
	Arginine/proline metabolism	.48E-01

(Supplementary Table 2), and mismatched controls were injected into 1-cell-stage embryos.

mRNA Injection

Human *GPER1* complementary DNA–containing plasmid (HsCD0032896) was transcribed with mMESSAGE mMACHINE (Ambion, Naugatuck, CT). Messenger RNA (mRNA) (200 μg) was injected into 1-cell-stage embryos.

Generation of gper1 Mutants

Transcription activator-like effector nuclease (TALENs) targeting *gper1* were obtained from Addgene (Watertown, MA) (TAL3272, TAL3273).[12] Adult TALEN-injected fish (F_0) were out-crossed with wild-type (WT) siblings, and progeny (F_1) were screened for somatic mutations by Sanger sequencing (Supplementary Table 3). F_1 mutants were out-crossed for at least 4 generations to avoid possible off-target effects.

Western Blot Analysis

Pooled larvae (n = 30–40) and cultured cells were processed for Western blot as previously described.[13] Antibodies are listed in Supplementary Table 4.

Whole-Mount In Situ Hybridization

Larvae were fixed, and in situ hybridization (ISH) was performed according to standard protocols.[14] *gper1* probe was generously gifted by David Volz.[15]

Liver Size Analysis

ISH images were obtained by brightfield microscopy, and *fabp10a*:GFP reporter larvae were imaged using fluorescence microscopy. Three-dimensional imaging of *fabp10a*:GFP fish was performed with a Yokogawa (Tokyo, Japan) W1 spinning disk confocal microscope. Image quantification was achieved using ImageJ (National Institutes of Health, Bethesda, MD) and Imaris software (Belfast, UK).

Histology and Immunohistochemistry of Zebrafish and Human Tissue

Zebrafish were fixed, sectioned, and processed with H&E stains as described.[16] For cell size analysis, zebrafish sections were stained with pan-cadherin and 4′,6-diamidino-2-phenylindole. Individual cell membrane staining was traced, and the cell area was measured with ImageJ. De-identified, formalin-fixed, paraffin-embedded human liver sections were obtained from the University of Utah (institutional review board no. 00091019; clinical characteristics summarized in Supplementary Tables 5 and 6) or from commercially available tissue arrays (OD-CT-DgLiv01-003; US Biomax, Derwood, MD) (Supplementary Table 6). Immunohistochemistry (IHC) (antibodies in Supplementary Table 4) and TUNEL staining were performed with established protocols.[14] GPER1 staining was scored by a pathologist (KJE).

Flow Cytometry and Cell Cycle Analysis

Fluorescence-activated cell sorting on *fabp10a*:GFP larvae was performed as previously described.[14] Cell cycle analysis was achieved with the BrdU Flow kit (BD Bioscience, San Jose, CA) and incubation in propidium iodide, followed by flow cytometry analysis, which was performed with FlowJo software (FlowJo, Ashland, OR).

Quantitative Reverse Transcription Polymerase Chain Reaction Analysis

RNA was isolated from zebrafish larvae, processed, and analyzed by quantitative reverse transcription polymerase chain reaction (qRT-PCR) as previously described.[17] Primers are listed in Supplementary Table 7.

Chemical Carcinogenesis

Age-matched *gper1*$^{-/-}$ or wild-type fish were exposed to 5 parts per million dimethylbenzanthrazene (DMBA) for 24 hours at 3, 4, and 5 weeks.[18] Chemical exposures commenced at 6 weeks (3 times/wk). Fish were monitored daily for survival and tumor formation until 33 weeks after DMBA treatment. Fish were killed upon reaching Institutional Animal Care and Use Committee–approved tumor limits or at 33 weeks after DMBA exposure. Histologic analysis was performed in a blinded fashion by a board-certified pathologist with expertise in zebrafish liver histology (KJE).

Steady-State Metabolomics Analysis

Adult livers were surgically removed and subjected to methanol extraction, as previously described.[17,19] Polar metabolites were identified with liquid chromatography–tandem mass spectrometry. Metabolic pathway analysis was performed with MetaboAnalyst (http://www.metaboanalyst.ca).

Figure 1. E2 increases liver size. (*A*) Brightfield and fluorescent images of male and female Tg(*fabp10a*:GFP) adult zebrafish exposed to DMSO (0.1%) or E2 (10 μmol/L) daily for 6 weeks. Scale bars, 2 mm. (*B*) Liver weight to body weight (%). (*C*) Transcriptomic analysis showing E2-induced up-regulated genes (fold change $>$ 10), particularly genes involved in the cell cycle. (*D*) Polar metabolomics showed significant sex-dimorphic differences between DMSO- and E2-exposed livers (fold change $\geq$ 2). (*E*) Liver size at 120 hpf determined by fluorescence microscopy in Tg(*fabp10a*:GFP) reporters and by ISH for *fabp10a*. Scale bars, 200 μm. Quantification of (*F*) *fabp10a* expression by qRT-PCR in Tg(*fabp10a*:GFP) larvae at 120 hpf, (*G*) liver volume by confocal microscopy, and (*H*) GFP$^+$ hepatocyte number by fluorescence-activated cell sorting. (*I*) Liver size after exposure to E2 (10 μmol/L), ANAS (10 μmol/L), and E2 + ANAS (10 μmol/L, 15 μmol/L) from 110 to 115 hpf (10 μmol/L). Scale bar, 50 μm. (*J*) Relative liver volume (fold change from DMSO), as assessed by confocal microscopy in Tg(*fabp10a*:GFP) larvae at 120 hpf. $\geq$3 independent experiments, except *C* and *D* represent 1 experiment with $\geq$3 biological replicates. Data are shown as mean ± standard error of the mean, numbers as indicated. *$P < .05$, **$P < .01$, ****$P < .0001$, 2-tailed Student *t* test. ANAS, anastrozole; FACS, fluorescence-activated cell sorting; M, mol/L.

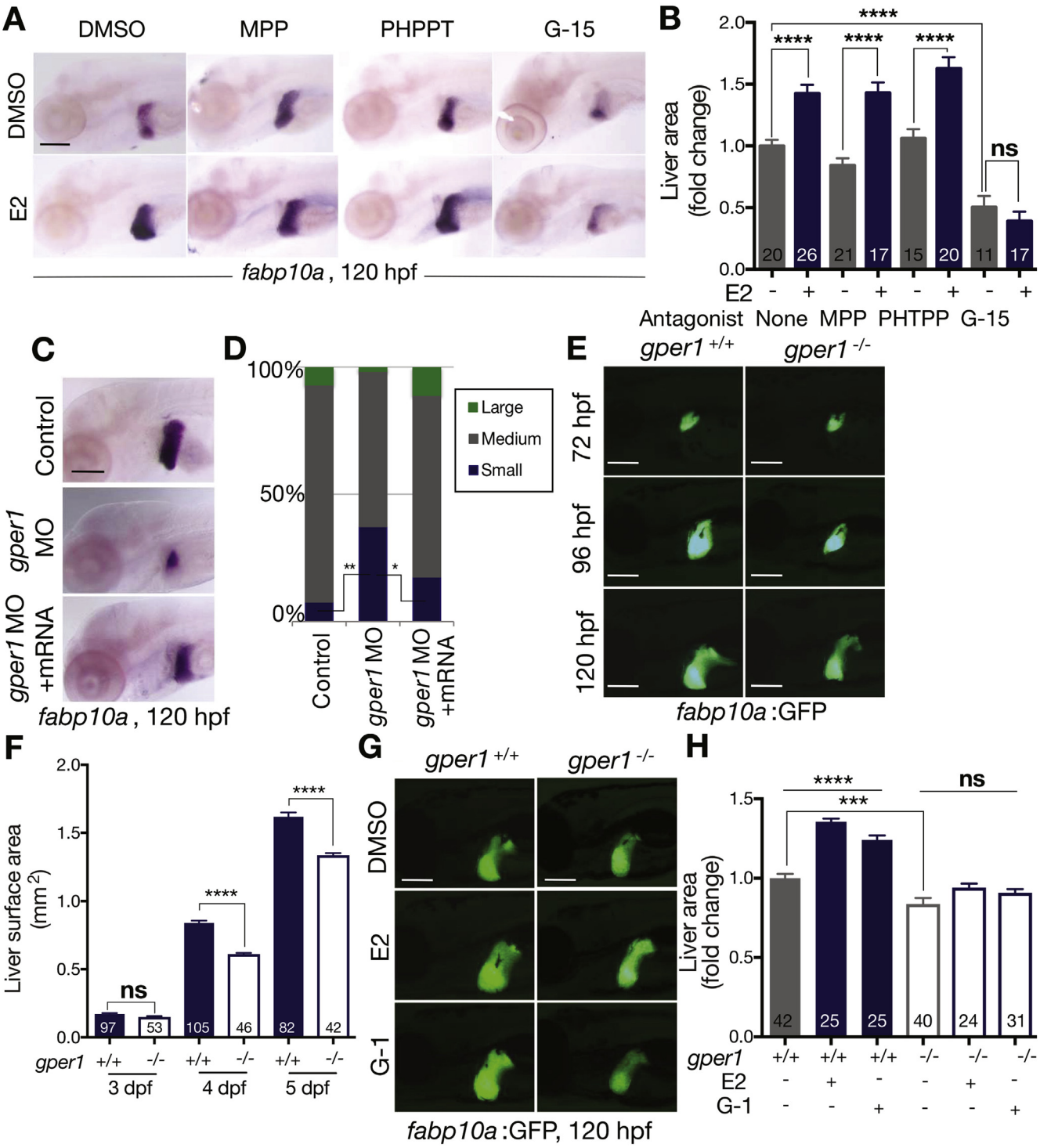

Figure 2. G-protein–coupled estrogen receptor 1 (GPER1) mediates the estrogenic effects on liver growth. (*A*) Liver size of larvae exposed to selective antagonists for ESR1 (MPP), ESR2 (PHTPP), or GPER1 (G-15) alone and with E2 from 110 to 115 hpf. (*B*) Liver area (fold change from DMSO). ****$P < .0001$, 2-tailed Student *t* test. (*C*) Liver size of WT, *gper1* morphants ± human *gper1* mRNA. (*D*) Relative liver size distribution. *$P < .05$, **$P < .01$, 2-tailed Student *t* test. (*E*) *gper1*$^{-/-}$;Tg(*fabp10a*:GFP) fish show progressively impaired liver development from 72 to 120 hpf. (*F*) Liver size of *gper1*$^{+/+}$ and *gper1*$^{-/-}$ larvae at 3, 4, 5 days post fertilization. ****$P < .0001$, 2-way analysis of variance (ANOVA). (*G*) *gper1*$^{-/-}$ mutants failed to respond to E2 or G-1. (*H*) Liver area (fold change from DMSO). ***$P = .0005$, ****$P < .0001$, 2-way ANOVA. Liver area assessed by ISH for *fabp10a* at 120 hpf. Values represent ≥3 independent experiments, mean ± standard error of the mean, numbers as indicated. Scale bars, 200 μm. ns, not significant.

Transcriptomic Analysis

RNA was extracted from resected livers, processed, and analyzed as previously described.[17] Gene Ontology terms were analyzed using DAVID (National Institutes of Health).

Results

Estrogen Enhances Liver Growth

To demonstrate the potential impact of endogenous estrogen levels on liver size, adult zebrafish livers were assessed in females and males. Livers of adult female zebrafish were bigger than those of male siblings, as visualized in hepatocyte reporter fish expressing green fluorescent protein (GFP) regulated by the fatty acid binding protein 10a promoter, Tg(*fabp10a*:GFP) (Figure 1*A*). Baseline liver-to-body weight ratios in 10 WT males and females at 7 months showed a significant 2.6-fold difference (Figure 1*B*). Because estrogen is one of the major sex hormones determining physiological differences between males and females, the potential impact of estrogen on liver growth was examined: zebrafish were exposed to E2 (10 μmol/L) or DMSO daily for 6 weeks, and liver size and weight were assessed in the context of total body length and mass (Figure 1*A* and *B*). Male livers responded more significantly to E2 with a 4.8-fold increase in liver-to-body weight ratio, whereas females exhibited a 1.6-fold enhancement (Figure 1*B*). These results suggest that liver mass is directly responsive to estrogen.

To uncover the signals by which E2 affects liver size, liver transcriptome analysis was performed with and without E2. Gene expression in male and female livers was different, with a subset of genes identified as *female-associated*, indicating genes up-regulated exclusively in females (Supplementary Figure 1*A*). These differences, however, are not solely due to estrogenic effects, because E2 did not simply convert the male liver transcriptome into one resembling a female transcriptome: in fact, E2 exposure altered transcriptional profiles in both sexes (Supplementary Figure 1*A*). Gene Ontology analysis showed that E2 enhanced the cell cycle and DNA metabolism-related gene expression (46 genes, $P = 3.4 \times 10^{-5}$), particularly in males (Figure 1*C* and Supplementary Figure 1*B* and *C*) (324 genes, $P = 7.4 \times 10^{-13}$). Given that the liver is a primary metabolic organ, we examined whether the sex and/or E2-associated increase in liver mass correlated with metabolic alterations, using steady-state metabolomics profiling (Figure 1*D* and Supplementary Figure 1*D* and *E*). Metabolite profiles were significantly different between males and females and were further altered by E2 exposure: metabolite set enrichment analysis showed that E2 exposure altered pyrimidine and purine metabolism in male livers, which is essential for DNA synthesis and cell proliferation (Figure 1*D*) (55 metabolites; pyrimidine, $P = 1.9 \times 10^{-8}$; purine, $P = 3.5 \times 10^{-3}$).[17] E2 altered metabolites involved in arginine/proline metabolism and RNA transcription in both male and female livers. Together, these findings indicate that E2 predominantly affects transcriptional programs and metabolites involved in cell cycling and proliferation.

To directly investigate the effect of E2 on hepatocytes, without the influence of pre-existing sex differences, zebrafish larvae were examined before sexual dimorphic features developed. Larvae were exposed to E2 for 5-hour intervals after hepatocytes were fully differentiated (>95 hpf). E2 increased liver size at 120 hpf as analyzed by ISH for *fabp10a*; this effect was confirmed by fluorescent imaging of hepatocyte reporters (Tg(*fabp10a*:GFP)) and qRT-PCR (Figure 1*E* and *F*) ($P < .01$). E2 also enhanced liver volume, by confocal microscopy (Figure 1*G*) ($P < .01$), and total hepatocyte number, as quantified by fluorescence-activated cell sorting (Figure 1*H*) ($P < .0001$). To determine the impact of endogenous E2, larvae were exposed to the aromatase inhibitor anastrozole, showing a decrease in liver size (Figure 1*I* and *J*). Critically, liver size could completely be rescued by escalating doses of exogenous E2 (Figure 1*J*) ($P < .01$). These results indicate that during larval stages, E2 regulates hepatocyte number and liver growth.

Estrogen Increases Liver Size via Activation of GPER1

To identify which receptor mediates the effect of E2 on liver growth, larvae were exposed to selective chemical antagonists for each estrogen receptor, MPP (ESR1),[20] PHTPP (ESR2),[21] and G-15 (GPER1),[22] alone and with E2. The E2-induced increase in liver size was specifically inhibited by coexposure with G-15, but not by ESR1 or ESR2 blockade (Figure 2*A* and *B*). Selective GPER1 activation with G-1 increased liver size and hepatocyte number, similarly to E2, whereas GPER1 inhibition with G-15 reduced liver size (Supplementary Figure 2*A* and *B*). Furthermore, knockdown of *gper1*, but not nuclear estrogen receptors *esr1, esr2a, esr2b*, or *esr2a* + *esr2b*, blocked the effect of E2 on liver growth, confirming specificity of the chemical modifiers (Supplementary Figure 2*C*). Importantly, human *GPER1* mRNA partially rescued the small liver phenotype in *gper1* morphants, showing specificity and evolutionary conservation (Figure 2*C* and *D*). Similarly, *GPER1* mRNA injection increased liver size in WT embryos but not after exposure to anastrozole, showing the concomitant importance of endogenous E2 for GPER1 activation (Supplementary Figure 2*D*). Finally, known environmental GPER1 agonists bisphenol A and tamoxifen likewise augmented liver size (Supplementary Figure 2*E* and *F*). To confirm that hepatic nuclear hormone receptor-mediated signaling was not significantly activated after E2 exposure, estrogen response element (ERE) reporter fish Tg(5xERE:GFP) were imaged to reflect DNA binding by nuclear hormone receptors.[23] Fluorescence imaging at 120 hpf showed that short exposure to E2 (110–115 hpf) had a moderate effect on baseline hepatic Esr signaling, whereas prolonged exposure for 24 hours significantly increased hepatic estrogen response element activity (Supplementary Figure 2*G* and *H*), consistent with the kinetics of nongenomic signaling vs genomic signaling

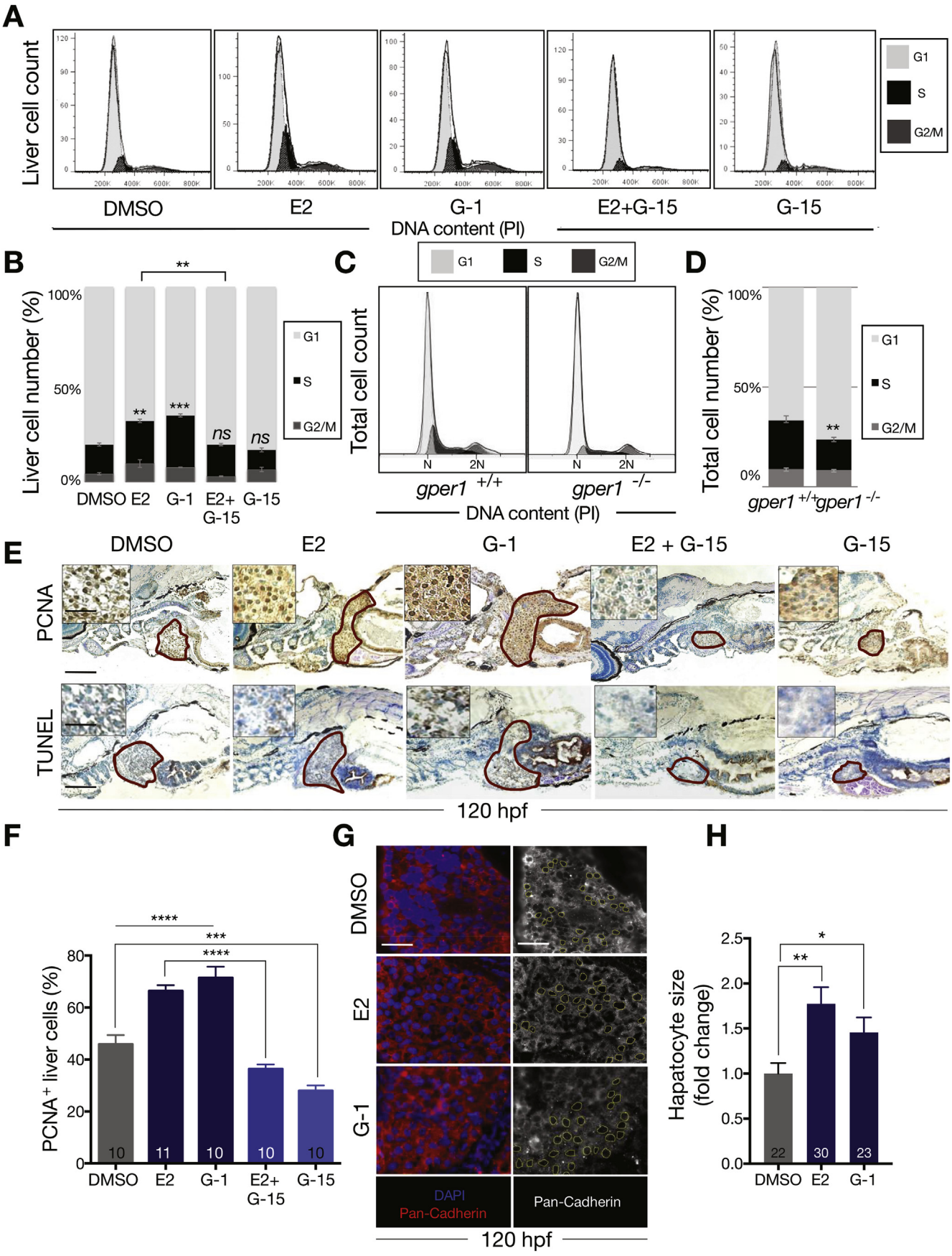
A
Liver cell count
DMSO
E2
G-1
E2+G-15
G-15
DNA content (PI)
G1
S
G2/M
B
Liver cell number (%)
100%
50%
0%
DMSO E2 G-1 E2+ G-15 G-15
**
***
ns
ns
C
Total cell count
N
2N
gper1 +/+
gper1 -/-
DNA content (PI)
D
Total cell number (%)
gper1 +/+ gper1 -/-
E
DMSO
E2
G-1
E2 + G-15
G-15
PCNA
TUNEL
120 hpf
F
PCNA+ liver cells (%)
****
***
****
10
11
10
10
10
G
DMSO
E2
G-1
DAPI
Pan-Cadherin
Pan-Cadherin
120 hpf
H
Hapatocyte size (fold change)
*
**
22
30
23

through transcriptional regulation. Intriguingly, *gper1* expression is dynamically regulated during development and is strongly localized to the liver at 72–120 hpf ,as determined by ISH and RT-PCR (Supplementary Figure 3*A*–*C*). Together, these data indicate that GPER1 affects E2-mediated liver growth during development.

To define the role of GPER1 in mediating E2-associated effects on liver growth, *gper1* mutant zebrafish were generated using TALENs: a 29-base pair deletion in exon 1 resulted in a premature stop codon, disrupting GPER1 protein production (Supplementary Figure 3*D* and *E*). GPER1 loss, assessed in the Tg(*fabp10a*:GFP) reporter background, impaired liver growth substantially after 96 hpf, but not earlier, supporting a requirement for E2 and GPER1 in liver outgrowth (Figure 2*E* and *F*). Consistent with these findings, the expression levels of hepatic progenitor markers *foxA3* and *prox1* were not affected in *gper1*$^{-/-}$ larvae at 48 or 72 hpf (Supplementary Figure 3*F* and *G*). Significantly, in contrast to WT livers, *gper1*$^{-/-}$ mutants did not respond to E2 or G-1 (Figure 2*G* and *H*), definitively indicating that E2 signals via GPER1 to increase liver size.

Estrogen activates GPER1 to promote cellular proliferation and cell cycle progression

To determine the cellular mechanism by which E2 enlarges liver size, cell cycle analysis was performed on propidium iodide-stained *fabp10a*:GFP^{+} hepatocytes at 120 hpf (Figure 3*A*). E2 and G-1 significantly increased hepatocytes in S and G2/M phase (S: 21.8%, G2/M: 9.4%) compared with controls (S: 14.9%, G2/M: 4.2%; $P < .01$); importantly, this effect was blocked by G-15 (Figure 3*B*) (S: 16.2%, G2/M: 2.9%; $P < .01$). In contrast, in *gper1*$^{-/-}$ mutants, whole-larvae cell cycle analysis at 120 hpf showed impaired cell cycle progression (S: 14.8%, G2/M: 8.1%; $P < .01$) compared with age-matched controls (Figure 3*C* and *D*) (S: 23.3%, G2/M: 8.5%). In WT embryos, cellular proliferation, marked by bromodeoxyuridine incorporation (Supplementary Figure 4*A* and *B*) and proliferating cell nuclear antigen (PCNA) staining, was enhanced after E2 or G-1 exposure (Figure 3*E* and *F* and Supplementary Figure 4*D* and *E*). This impact was not sustained, however, because 45 hours after E2 exposure, cell cycle parameters and bromodeoxyuridine incorporation were comparable to those of controls (Supplementary Figure 4*C*–*E*). In contrast, G-15 decreased PCNA^{+} hepatocytes in WT embryos and inhibited E2-induced increases. Any impact of E2 on hepatocyte viability was excluded by TUNEL staining (Figure 3*E* and Supplementary Figure 4*F*). Cell-size alterations contributing to organ size were examined by pan-cadherin immunostaining, showing a significant 50% increase in hepatocyte area upon E2 and G-1 exposure (Figure 3*G* and *H*). These results indicate that E2 promotes hepatocyte proliferation, cell cycle progression, and overall size via GPER1, leading to increased liver mass.

Estrogen Signals Through GPER1 to Stimulate the PI3K-Akt Pathway

To determine the downstream signals by which GPER1 enhances liver growth, a targeted approach was used, based on prior work indicating that many G-protein–coupled receptors activate PI3K signaling.[24] To define a potential interaction between GPER1 and PI3K-Akt signaling, larvae were exposed to the PI3K inhibitor LY292002, PI3K activator 740Y-P, and Akt inhibitor MK-2206. Coexposure with either LY292002 or MK-2206 diminished E2-induced liver growth (Figure 4*A* and *B* and Supplementary Figure 5*A*). MK-2206 also decreased liver size in WT and *gper1*$^{-/-}$ mutants, suggesting that E2/GPER1-PI3K/Akt signaling is essential for larval liver outgrowth. In contrast, activation of PI3K signaling by 740Y-P increased liver size in WT larvae and rescued *gper1* morphants or mutants (Figure 4*A* and *B* and Supplementary Figure 5*B*). Cell proliferation as measured by PCNA was decreased by MK-2206 and increased with 740Y-P, respectively (Supplementary Figure 5*C* and *D*). Because PI3K can activate both Akt and mitogen-activated protein kinase (MAPK)–extracellular signal–regulated kinase (Erk) pathways, mitogen-activated protein kinase–Erk signaling was also examined. Western blot for phosphorylated (p-) Akt and p-Erk showed that E2 increased p-Akt with minimal effects on p-Erk (Figure 4*C*). *gper1*$^{-/-}$ mutants exhibited decreased baseline p-Akt levels compared with the WT, which was restored by 740Y-P exposure. These data show that E2-GPER1 activates the PI3K-Akt pathway to increase liver growth.

Estrogen Activates the mTORC1 Pathway via GPER1 to Increase Liver Size

To determine the effector of E2-GPER1-mediated activation of PI3K-Akt signaling, the role of the mTOR complex 1 (mTORC1) was investigated. Coexposure with the mTORC1 inhibitor rapamycin diminished the enlarged liver induced by E2 or G-1 (Supplementary Figure 5*E* and *F*). Similarly, *mtor* knockdown decreased liver size and blocked

Figure 3. E2 signals via GPER1 to promote cell cycle progression, proliferation, and cell size increase in the liver. (*A*) FACS profiles of cell cycle analysis of GFP^{+} hepatocytes in Tg(*fabp10a*:GFP) larvae. (*B*) Relative distribution of GFP^{+} hepatocytes in G1 (*light gray*), S (*black*), or G2/M (*dark gray*). Asterisks indicate difference in S and G2/M phase vs DMSO-exposed hepatocytes: $^{**}P < .01$, $^{***}P < .001$, 2-tailed Student *t* test. (*C*, *D*) Cell-cycle analysis showed decreased S phase in *gper1*$^{-/-}$ mutants at 120 hpf. $^{**}P < .01$, 2-tailed Student *t* test. (*E*) PCNA (*top panel*) and TUNEL (*bottom panel*) staining of whole larvae section. Liver outline in red. Insets show higher magnification of hepatocytes. Scale bars, 100 μm; scale bar (inset), 30 μm. (*F*) Percentage of PCNA^{+} cells from total hepatocytes in the liver area. $^{***}P < .001$, $^{****}P < .0001$, 2-tailed Student *t* test; $^{****}P < .0001$, 1-way ANOVA. (*G*) Liver sections of DMSO-, E2-, or G-1–exposed larvae stained with DAPI (*blue*) and pan-cadherin (*red*). Scale bars, 25 μm. (*H*) Hepatocyte size quantification based on pan-cadherin staining and cell area (fold change from DMSO). $^{*}P < .05$, $^{**}P < .01$, 2-tailed Student *t* test. Mean of 3 independent experiments ± standard error of the mean, numbers as indicated. DAPI, 4′,6-diamidino-2-phenylindole; FACS, fluorescence-activated cell sorting; ns, not significant; PI, propidium iodide.

the effect of E2 (Supplementary Figure 5*G* and *H*). Hypomorphic *mtor*$^{-/-}$ mutants[25] exhibited smaller livers that did not respond to E2 or G-1 (Figure 4*D* and *E*), indicating that GPER1 acts upstream of mTORC1. Finally, Western blot of mTORC1 target ribosomal protein S6 showed increased phosphorylation with E2 and G-1 (Figure 4*F*); importantly,

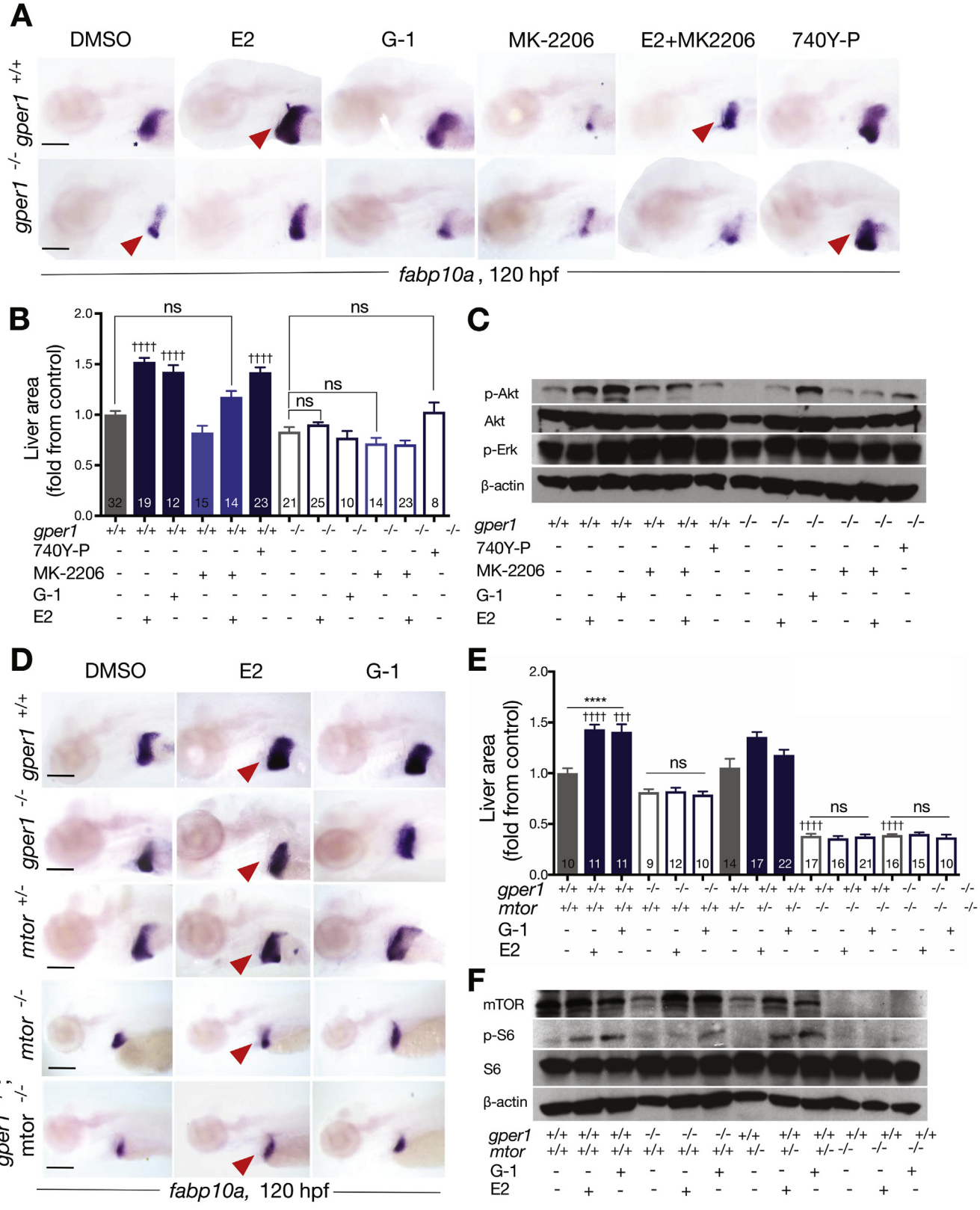

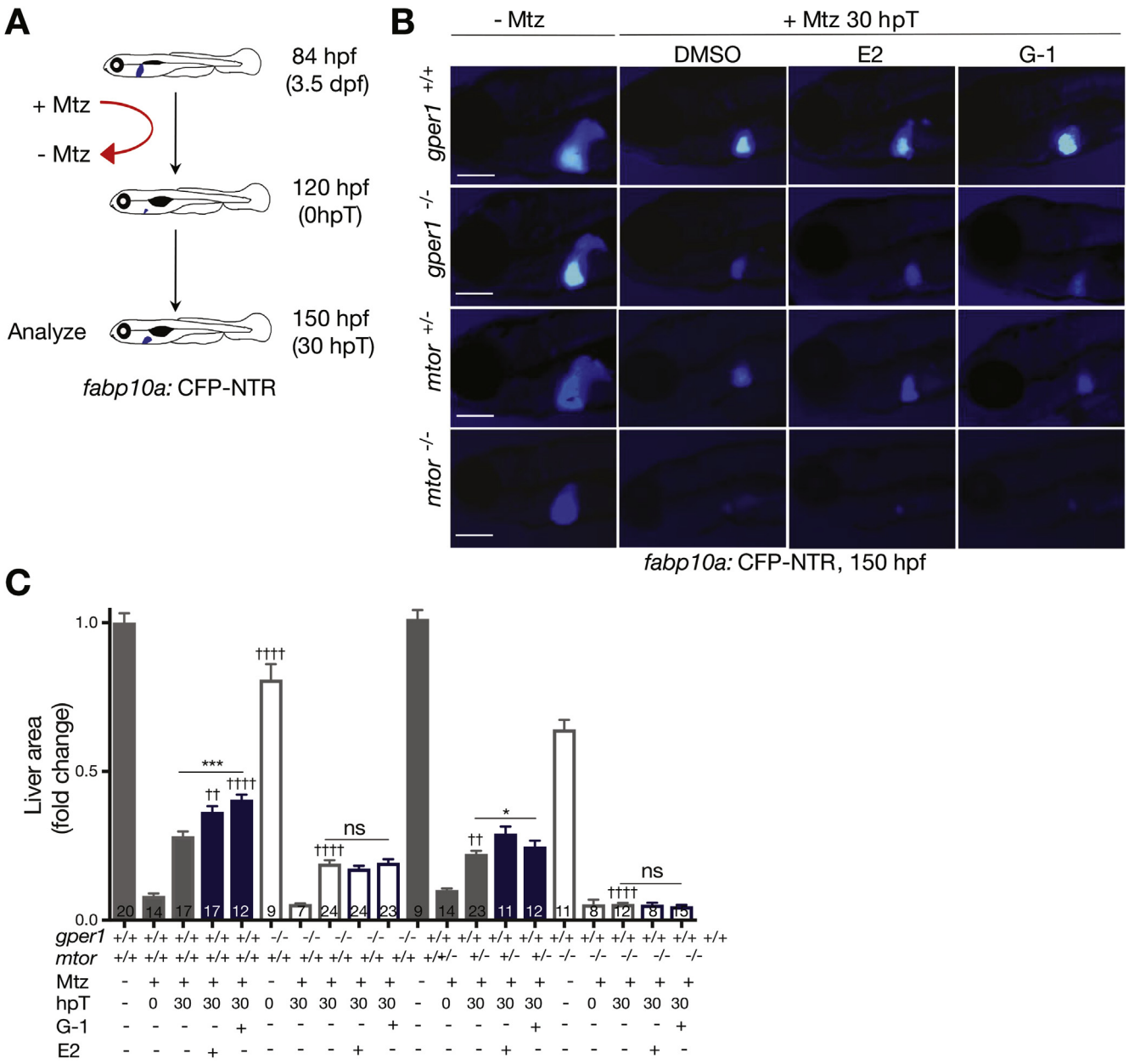

Figure 5. E2 promotes liver regeneration via activation of the GPER1 and mTORC1 pathways. (*A*) Scheme for Mtz exposure and liver regeneration analysis. (*B*) *gper1*$^{+/+}$, *gper1*$^{-/-}$, *mtor*$^{+/-}$, and *mtor*$^{-/-}$ larvae in Tg(*fabp10a:*CFP-NTR) background at 150 hpf. Scale bars, 200 μm. (*C*) Liver area (fold change from –Mtz WT) as determined by cyan fluorescent protein expression. Dagger symbol (†) indicates significant difference from Mtz-treated WT at 30 hours after treatment: $^{\dagger\dagger}P < .005$, $^{\dagger\dagger\dagger\dagger}P < .0001$, 2-way ANOVA. ns, not significant.

IHC staining localized increased p-S6 to the liver (Supplementary Figure 5*I*). These effects were abolished in *gper1*$^{-/-}$ and *mtor*$^{-/-}$ mutants (Figure 4*F*). Together, these functional and biochemical analyses show that E2-GPER1–dependent regulation of liver size is mediated by activation of PI3K-mTORC1.

Figure 4. E2 signals via GPER1 to stimulate PI3K/mTORC1 to increase liver size. (*A*) Liver size in *gper1*$^{+/+}$ and *gper1*$^{-/-}$ larvae. E2-induced liver size increase was blocked by E2+MK-2206 coexposure (*top row, arrowheads*). Smaller liver in *gper1*$^{-/-}$ mutants was normalized by 740Y-P (*bottom row, arrowheads*). (*B*) Liver area (fold change from DMSO). Dagger symbol (†) indicates difference from DMSO-exposed liver: $^{\dagger\dagger\dagger\dagger}P < .0001$, 2-way ANOVA. (*C*) Immunoblot analysis of *gper1*$^{+/+}$ and *gper1*$^{-/-}$ whole larvae. (*D*) E2 or G-1 exposure increased liver size in *gper1*$^{+/+}$ and *mtor*$^{+/-}$ but not in *gper1*$^{-/-}$, *mtor*$^{-/-}$, or *gper1*$^{-/-}$;*mtor*$^{-/-}$ larvae (*red arrowheads*). (*E*) Liver area (fold change from DMSO). $^{****}P < .0001$, 2-way ANOVA. (*F*) Immunoblot analysis of *gper1*$^{+/+}$, *gper1*$^{-/-}$, *mtor*$^{+/-}$, and *mtor*$^{-/-}$ whole larvae. Results represent ≥3 independent experiments. Representative blots of ≥5 independent experiments. Liver area was assessed by ISH for *fabp10a* at 120 hpf. Mean ± standard error of the mean, numbers as indicated. All scale bars, 200 μm. ns, not significant.

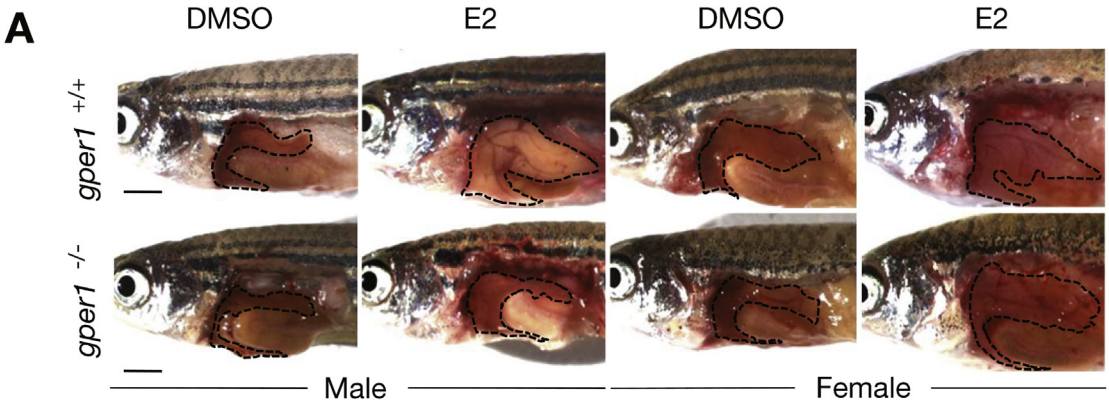
A
DMSO
E2
DMSO
E2
gper1 +/+
gper1 -/-
Male
Female

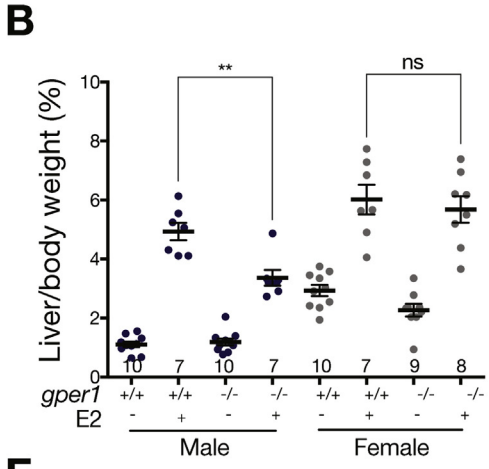
B
Liver/body weight (%)
**
ns
gper1
E2
Male
Female

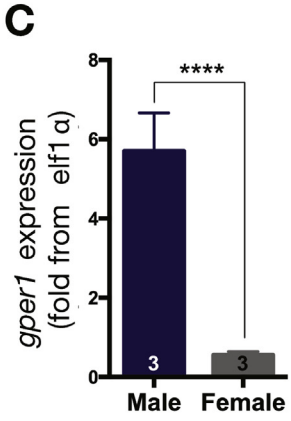
C
gper1 expression (fold from elf1α)
****
Male
Female

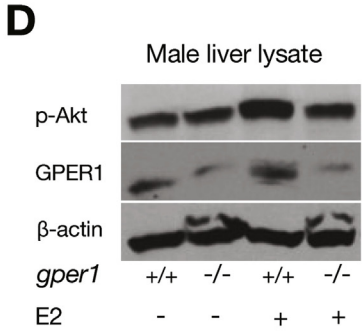
D
Male liver lysate
p-Akt
GPER1
β-actin
gper1
E2

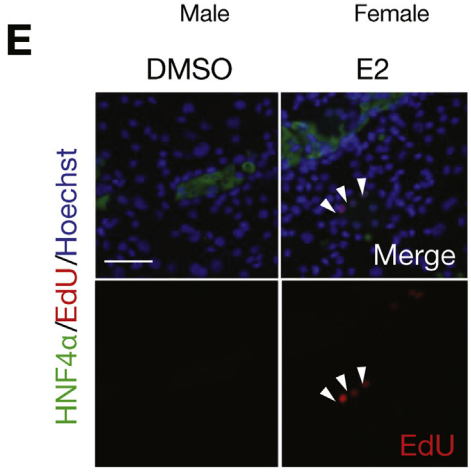
E
DMSO
E2
HNF4α/EdU/Hoechst
Merge
EdU

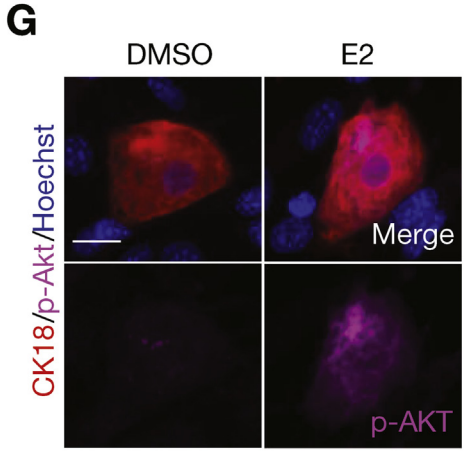
G
DMSO
E2
CK18/p-Akt/Hoechst
Merge
p-AKT

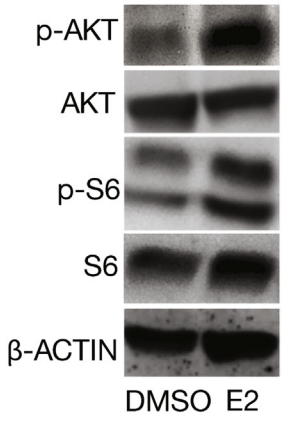
I
p-AKT
AKT
p-S6
S6
β-ACTIN
DMSO E2

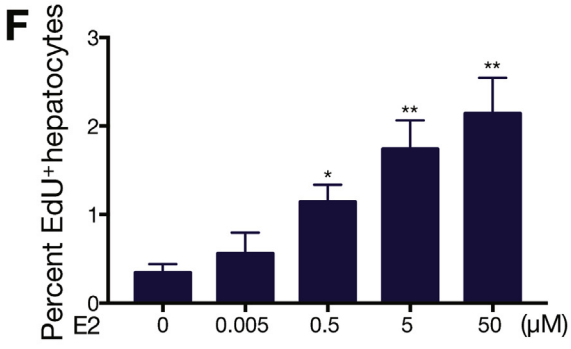
F
Percent EdU+ hepatocytes
E2
0
0.005
0.5
5
50
(μM)

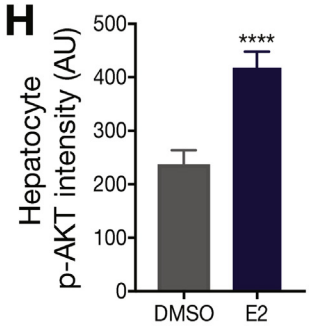
H
Hepatocyte p-AKT intensity (AU)
****
DMSO
E2

Estrogen Promotes Liver Regeneration via Activation of GPER1 and mTORC1 Pathways

Our previous work indicated strong conservation of developmental regulatory signals in liver regeneration.[13,14] To determine whether the GPER1-mTOR pathway affects liver repair, a genetic ablation strategy was used: expression of bacterial nitroreductase in hepatocytes (Tg(*fabp10a:CFP-NTR*)) enables targeted ablation upon metronidazole (Mtz) exposure.[26] Larvae were exposed to Mtz from 84 to 120 hpf, followed by chemical incubation and liver assessment at 30 hours after treatment (Figure 5*A*). E2- or G-1–exposed larvae showed significantly more liver regrowth compared with controls (Figure 5*B* and *C*) ($P < .01$, $P < .0001$). In contrast, *gper1*$^{-/-}$ mutants exhibited significantly less regrowth ($P < .0001$), which was not enhanced by E2 or G-1 (Figure 5*B* and *C*). These results indicate that E2-GPER1 signaling promotes liver growth after injury.

To confirm the role of the E2/GPER1-PI3K/mTOR axis during liver repair, compound *mtor*$^{-/-}$*;fabp10a:CFP-NTR* fish were examined. Liver regrowth in *mtor*$^{-/-}$ mutants was significantly reduced compared with controls ($P < .0001$) and was not enhanced by E2 or G-1 exposure (Figure 5*B* and *C*), highlighting a general requirement for mTOR during liver regeneration and its requirement for mediating the effect of E2. IHC showed lower p-S6 levels in livers of both *gper1*$^{-/-}$ and *mtor*$^{-/-}$ mutants after injury, indicating a failure to up-regulate mTORC1 signaling upon hepatocyte ablation (Supplementary Figure 6*A* and *B*). Collectively, our data show a direct connection between E2 and mTORC1 in promoting liver growth during regeneration.

GPER1 Mediates Adult Liver Growth

Because E2-GPER1 promotes liver growth and repair in zebrafish larvae, it may influence adult liver biology, as implied in our initial observations (Figure 1). Steady-state liver weight and liver-to-body weight ratios in WT and *gper1*$^{-/-}$ males were not significantly different (Figure 6*A* and *B* and Supplementary Figure 6*C*); in contrast, E2 induced an elevation in male liver weight that was significantly reduced in *gper1*$^{-/-}$ mutants (Figure 6*A* and *B*), indicating sensitivity to exogenous E2 that may be contributed to by a 6-fold increase in *gper1* expression in male over female livers (Figure 6*C*). In contrast, loss of *gper1* in females reduced liver weight and liver-to-body weight ratios (Figure 6*A* and *B*), and inhibition of endogenous estrogen production by anastrozole also reduced female liver-to-body weight ratios in WT, but not in *gper1*$^{-/-}$, mutants (Supplementary Figure 6*F* and *G*). In addition, body weight and length measurements showed a systemic effect of GPER1 loss in both sexes, consistent with the importance of mTOR for metabolic homeostasis (Supplementary Figure 6*D* and *E*). Furthermore, comparison of all parameters between WT and *gper1*$^{-/-}$ animals also suggests an impact of E2 on liver weight and whole body weight and length independent of GPER1 signaling, likely through ESR activity. Increased levels of p-Akt after 5 hours of E2 exposure in WT male livers, but not those of *gper1*$^{-/-}$, mutants (Figure 6*D*) further highlights the persistence of the E2-GPER1-PI3K-Akt regulatory axis in adults.

GPER1 Promotes Human Hepatocyte Growth

To show that the pro-proliferative effects of E2 have relevance to human physiology, a human primary hepatocyte coculture system was used.[27] E2 increased proliferation in male hepatocytes, doubly labeled with hepatocyte nuclear factor 4α (HNF4α) and ethynyldeoxyuridine, in a concentration-dependent manner (Figure 6*E* and *F*) ($P < .01$). Furthermore, E2 exposure enhanced p-AKT and p-S6 levels (Figure 6*G–I*). *GPER1* is expressed in human hepatocytes but not in the cocultured support cells (Supplementary Figure 6*H*), indicating a cell-autonomous effect of E2/GPER1 on hepatocyte proliferation. In human HepG2 cells, E2-associated increases in p-AKT and p-S6 were blocked by G-15 coexposure (Supplementary Figure 7*A*), highlighting the fact that E2 similarly signals via the Akt-mTOR pathway in human liver cancer. Together, these results show the conserved role of E2-GPER1-PI3K-Akt-mTOR in promoting human hepatocyte proliferation.

GPER1 Expression Marks Human Cirrhotic Liver and HCC

To assess the potential clinical relevance of GPER1 activity in human liver, GPER1 expression was quantified in samples from 68 individual patients: 30% of noncirrhotic livers exhibited patchy to diffuse GPER1 staining (Figure 7*A* and *B*, and Supplementary Figure 7*B*, and Supplementary Tables 5 and 6) (staining score $\geq$ 1+). GPER1 was expressed at higher levels in normal male livers than female livers, consistent with the zebrafish analysis (Supplementary Figure 7*B* and *C*). In contrast, 91% of cirrhotic livers and 86% of HCC samples exhibited positive

Figure 6. E2 signaling via GPER1 promotes sex dimorphism in adult liver growth. (*A*) Adult *gper1*$^{+/+}$ and *gper1*$^{-/-}$ exposed to DMSO or E2. Scale bars, 2 mm. (*B*) Liver weight/body weight (%). $^{**}P < .0001$, 2-way ANOVA. (*C*) Sex-specific *gper1* liver expression (vs *elf1*α). $^{****}P < .0001$, 2-tailed Student *t* test. (*D*) Immunoblot for p-Akt, GPER1, and β-actin levels in *gper1*$^{+/+}$ and *gper1*$^{-/-}$ male livers. (*E*) Immunofluorescent staining of DMSO- or E2-exposed male donor-derived hepatocytes with EdU (*red*) and HNF4α (*green*). White arrowheads indicate EdU and HNF4α double-positive cells. Scale bar, 100 μm. (*F*) Percentage of EdU^{+} hepatocytes. Asterisks indicate significant difference from DMSO controls: $^{*}P < .05$, $^{**}P < .01$, 2-tailed Student *t* test. (*G*) Immunofluorescent staining of DMSO or E2-exposed primary hepatocytes with p-Akt (*pink*) and CK18 (*red*). (*H*) Quantification of p-Akt intensity (AU) in DMSO or E2-treated hepatocytes. $^{****}P < .0001$, 2-tailed Student *t* test. (*I*) Immunoblot for p-AKT, AKT, p-S6, S6, and β-actin levels in DMSO- or E2-exposed male donor-derived hepatocytes. Results represent $\geq$3 independent experiments, mean $\pm$ standard error of the mean, numbers as indicated. AU, arbitrary unit; EdU, ethynyldeoxyuridine; HNF4α, hepatocyte nuclear factor 4α; M, mol/L; ns, not significant.

patchy to diffuse cytoplasmic GPER1 staining, with enhanced reactivity of hepatocytes around portal tracts and fibrous bands (Figure 7*A* and *B*) (noncirrhotic vs cirrhotic, $P < .05$). These results indicate that GPER1 is increasingly expressed in cirrhotic livers and HCC, implying a potential role for GPER1 in human hepatocarcinogenesis.

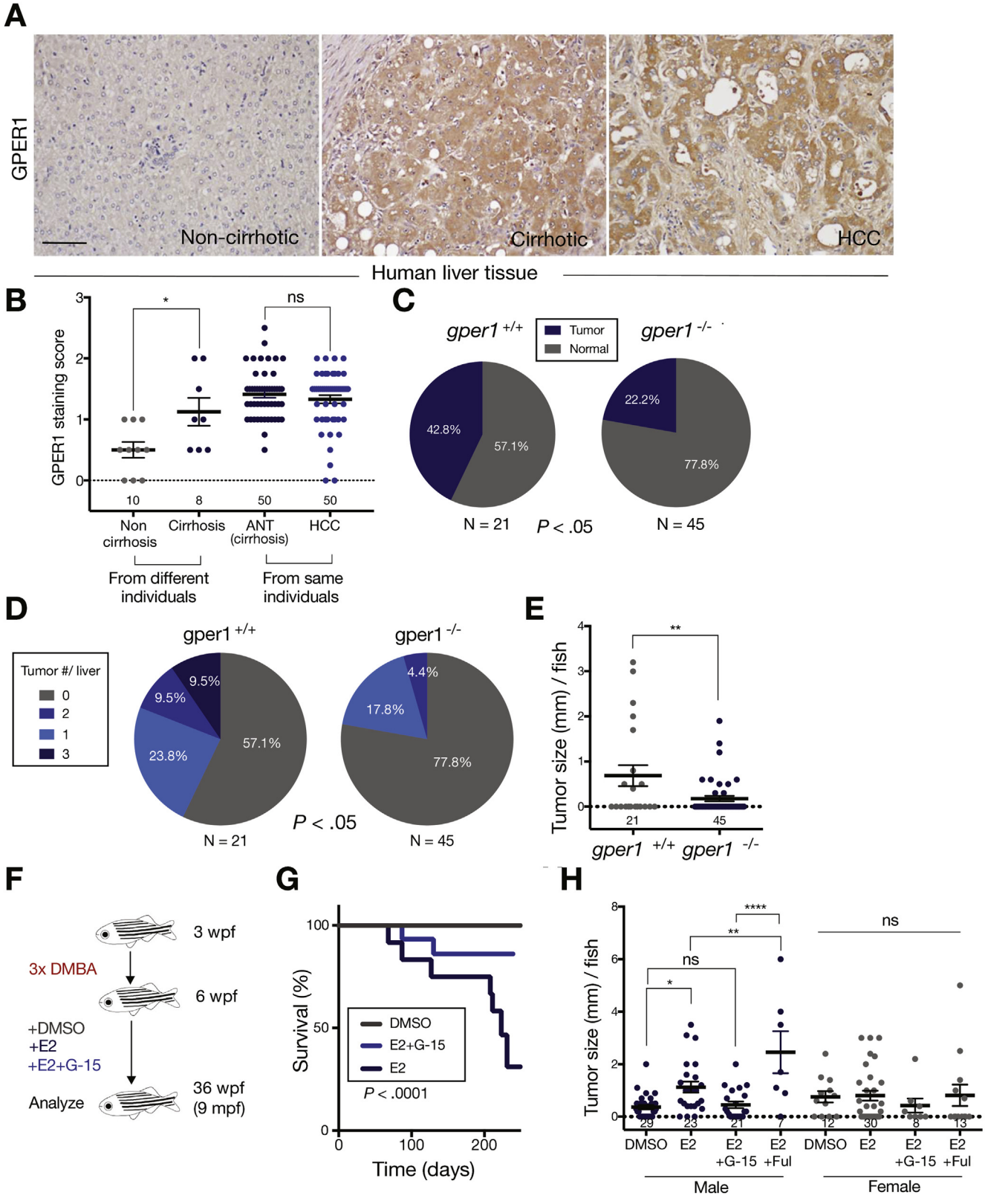

GPER1 Contributes to Sex Dimorphism in Cancer Formation and Progression

Dysregulation of signaling pathways controlling embryonic development and adult tissue homeostasis are frequently causative in carcinogenesis.[28,29] Given the role of E2-GPER1 in liver growth and its elevation in human liver cancer samples, its impact on cancer formation was examined in a well-established model of chemical liver carcinogenesis with DMBA:[18] *gper1*$^{-/-}$ mutants exhibited a significant 50% reduction in liver cancer incidence compared with DMBA-treated controls (Figure 7*C*) (42.8%, $n = 21$ vs 22.2%, $n = 45$; $P < .05$): tumor number per liver as a measure of tumor initiation in the entire cohort was decreased in *gper1*$^{-/-}$ mutants (Figure 7*D*) ($P < .05$). Moreover, average liver tumor size, as an indicator of tumor progression, was decreased by >70% in *gper1*$^{-/-}$ mutants (Figure 7*E*) (0.7 vs 0.2 mm, $P < .01$). These results imply that GPER1 function directly influences both the initiation and progression of liver cancer, suggesting a possible therapeutic role for receptor blockade.

To determine if E2-GPER1 is a possible therapeutic target in liver carcinogenesis, DMBA-exposed fish were subsequently treated 3 times weekly with DMSO, E2, or E2 + G-15 (Figure 7*F*). Significantly, E2-exposed fish had decreased survival compared with controls and those concomitantly exposed to E2 + G-15 (Figure 7*G*) ($P < .0001$). E2 exposure almost doubled liver tumor growth at 33 weeks after carcinogenesis, as indicated by larger overall tumor size (Supplementary Figure 7*D*) (mean 0.5 vs 0.9 mm, $P < .01$). Strikingly, G-15 coexposure reduced the E2-associated increase in tumor burden to below baseline levels (0.9 vs 0.4 mm, $P = .01$). Importantly, the ESR antagonist fulvestrant in combination with E2 did not decrease tumor size (Figure 7*H* and Supplementary Figure 7*D*) but, rather, caused an increase in tumor size in both sexes. Consistent with the known agonistic potential of selective ESR inhibitors on GPER1,[30] fulvestrant exposure increased total and phosphorylated Akt in zebrafish larvae (Supplementary Figure 7*E*). Histologic analysis showed the presence of hepatocellular adenoma, HCC, and cholangiocarcinoma without the chemical treatments affecting the overall tumor spectrum (Supplementary Figure 7*F* and *G*). Sex-stratified analysis showed that E2 effectively tripled tumor size in males ($P < .001$) (Figure 7*H* and Supplementary Figure 7*D*); likewise, blockade by G-15 predominantly reduced tumor size in males ($P < .05$), with less impact in female fish. Fulvestrant enhanced tumor size, particularly in males ($P < .001$). Together, these results indicate that GPER1 is an essential component of the sexually dimorphic response to E2 during liver growth, including carcinogenesis, which may have therapeutic relevance for the detection and treatment of human liver disease.

Discussion

Liver cancer is the second most common cause of cancer death worldwide, and it predominantly affects men.[2] Here, we identified a novel role for GPER1 in hepatocytes that cell-autonomously regulates larval liver growth and contributes to the sex dimorphisms observed in liver cancer incidence and growth. E2 promotes hepatocyte cell cycle progression and proliferation through GPER1 and downstream activation of PI3K-mTOR signaling. Importantly, the GPER1-mTOR pathway remains essential for liver repair. Prospective in vivo longitudinal carcinogenesis assays identify GPER1 as an important factor promoting E2-mediated liver cancer initiation and progression. Sex stratification analysis shows a male-predominant effect. Although ESR inhibition worsens outcome, preclinical studies with a selective GPER1 antagonist highlight the therapeutic potential of GPER1 blockade for liver cancer treatment. Likewise, increased GPER1 expression in human cirrhotic livers and HCC indicate its possible utility as a biomarker for disease progression.

The mTOR pathway is essential for organ size regulation,[31] functioning as a growth checkpoint that tightly coordinates cell growth with environmental cues, such as cellular stress, energy status, and amino acid availability.[29] Here, to our knowledge, we report a previously unidentified role of E2-GPER1 acting upstream of mTORC1 to promote hepatocyte proliferation and liver growth. We further identify the impact of E2-GPER1 activation on pyrimidine and purine metabolism, supporting recent work that mTORC1 is essential for de novo pyrimidine and purine biosynthesis to meet the anabolic demands of rapidly proliferating cells.[32,33] Prior studies have reported sexually dimorphic mTOR activity in the liver.[34,35] Our study is the first to elucidate how hepatic mTOR may sense a sex-specific environment through GPER1 and influence liver growth.

Several clinical and laboratory studies have shown sexually dimorphic responses after hepatectomy, with females being more tolerant and having a higher rate of liver

Figure 7. E2 signaling promotes liver cancer initiation and progression via GPER1. (*A*) Human noncirrhotic liver, cirrhotic liver, and HCC sections immunostained for GPER1 in. Scale bar, 100 μm. All values represent mean ± standard error of the mean, numbers as indicated. (*B*) Quantification of GPER1 staining scores of noncirrhotic livers; cirrhotic livers; adjacent nontumor (ANT) tissues, which are mostly cirrhotic; and HCC tissues. Numbers as indicated, mean ± standard error of the mean. *$P < .05$, 2-tailed Mann-Whitney test. (*C*) Total liver cancer incidence in DMBA-exposed adults at 7 months after fertilization was reduced by 50% in *gper1*$^{-/-}$ mutants compared with the WT. $P < .05$, 1-tailed chi-squared test. (*D*) Number of liver tumors per fish was decreased in *gper*$^{-/-}$ mutants. *$P < .05$, 1-tailed Mann–Whitney test. (*E*) Tumor size (mm) per fish. **$P < .01$, 2-tailed Student *t* test. (*F*) Scheme illustrating DMBA carcinogenesis followed by chemical prevention trial. (*G*) Kaplan–Meier survival plot. n = 52, 66, and 39 for DMSO-, E2-, and E2 + G-15–treated adults, respectively, at 249 days after first treatment. $P < .0001$, log-rank (Mantel–Cox) test. (*H*) Liver tumor size (mm) per fish at 9 months after fertilization . *$P = .0172$, **$P = .0053$, ****$P < .0001$, 1-way ANOVA, stratified by sex. ns, not significant.

regeneration.[36] E2 levels reportedly increase after liver injury[37] and improve impaired liver regeneration in ovariectomized female mice.[38] The mechanisms involved, however, had been incompletely understood. Here, we show that E2 specifically activates GPER1 and mTORC1 to promote liver regrowth after injury. The importance of E2 can be gleaned from clinical observations: E2 levels rapidly increase after liver resection in patients.[5] Furthermore, pregnancy is associated with hepatomegaly,[39] and gestational E2 increase enhances liver repair,[40] suggesting a physiological benefit for E2 during periods of liver growth. Indeed, *gper1*$^{-/-}$ mutants exhibit significantly delayed liver outgrowth during development and after injury. Nevertheless, *gper1*$^{-/-}$ mutants have a greater capacity for liver regeneration compared with *mtor*$^{-/-}$ mutants, indicating that E2-GPER1 is one among several inputs integrated by mTOR to regulate liver regeneration. We postulate that GPER1 mediates E2 activation of PI3K-mTOR in a sex-dimorphic fashion to promote liver regeneration.

Sexual dimorphism in liver cancer has long been documented, but a detailed mechanistic understanding has not been established. Both protective and tumor-promoting effects for E2 have been reported: E2-mediated reduction of inflammatory cytokines, such as IL-6 in liver-resident immune cells, appears to inhibit tumorigenesis.[41,42] Several other studies have shown liver tumor-promoting properties of E2.[43,44] Clinical trials in HCC patients with the ESR antagonist tamoxifen have been disappointing;[45,46] in fact, tamoxifen increased the size and number of hepatic lesions.[47] Tamoxifen and fulvestrant, used in our study, were subsequently found to be agonists for GPER1,[7,30,48] explaining the negative clinical results, consistent with our data for fulvestrant inducing Akt phosphorylation in vivo and increasing liver tumor burden. These findings are of particular importance because men with cirrhosis have persistently elevated serum levels of E2, and these patients are at highest risk for developing liver cancer. Our results definitively show a growth-promoting role for E2 in liver cancer acting in hepatocytes through GPER1; further studies are needed to define the various and likely receptor- and cell-type–specific influences of E2 on inflammation in the context of liver cancer.

The involvement of GPER1-PI3K-mTOR signaling in hepatocyte proliferation and organ growth prompted us to hypothesize that GPER1 may promote liver carcinogenesis. Indeed, activation of PI3K-Akt (approximately 70%) and mTORC1 (approximately 45%) pathways is found in HCC and positively correlates with tumor metastasis, recurrence, and poor prognosis.[49,50] Genetic alterations of PI3K/mTOR pathway components are found at lower frequencies in HCC: exome sequencing showed mutation frequencies in PIK3CA ($\leq$2%), mTOR ($\leq$2%), TSC1/TSC2 ($\leq$5%), and PTEN ($\leq$3%).[51,52] In the context of our data, it is tempting to speculate that PI3K-mTOR activity in HCC may instead depend on upstream ligand activation, mediated by increased E2 levels and GPER1 expression in cirrhotics, as also observed by Wei et al. [41] Because >80% of HCC patients are diagnosed at late stages without hope for cure, there is an urgent need for earlier detection and targeted therapeutic interventions. The pro-proliferative consequences of E2-GPER1 activation of PI3K-mTOR signaling, together with our in vivo data showing strong responses to GPER1 antagonist treatment in both cancer initiation and progression, clearly indicate that drugs targeting E2-GPER1 may offer exciting new therapeutic applications in liver cancer prevention and treatment.

Supplementary Material

Note: To access the supplementary material accompanying this article, visit the online version of *Gastroenterology* at www.gastrojournal.org, and at https://doi.org/10.1053/j.gastro.2019.01.010.

References

1. Ferlay J, Soerjomataram I, Dikshit R, et al. Cancer incidence and mortality worldwide: sources, methods and major patterns in GLOBOCAN 2012. Int J Cancer 2015; 136:E359–E386.
2. Sato N, Lindros KO, Baraona E, et al. Sex difference in alcohol-related organ injury. Alcohol Clin Exp Res 2001; 25:40S–45S.
3. Guéchot J, Peigney N, Ballet F, et al. Sex hormone imbalance in male alcoholic cirrhotic patients with and without hepatocellular carcinoma. Cancer 1988;62:760–762.
4. Castagnetta LAM, Agostara B, Montalto G, et al. Local estrogen formation by nontumoral, cirrhotic, and malignant human liver tissues and cells. Cancer Res 2003; 63:5041–5045.
5. Francavilla A, Panella C, Polimeno L, et al. Hormonal and enzymatic parameters of hepatic regeneration in patients undergoing major liver resections. Hepatology 1990; 12:1134–1138.
6. Barros RPA, Gustafsson J-Å. Estrogen receptors and the metabolic network. Cell Metab 2011;14:289–299.
7. Filardo EJ, Quinn JA, Bland KI, et al. Estrogen-induced activation of Erk-1 and Erk-2 requires the G protein-coupled receptor homolog, GPR30, and occurs via trans-activation of the epidermal growth factor receptor through release of HB-EGF. Mol Endocrinol 2000; 14:1649–1660.
8. **Haas E**, **Bhattacharya I**, **Brailoiu E**, et al. Regulatory role of G protein-coupled estrogen receptor for vascular function and obesity. Circ Res 2009;104:288–291.
9. Deschamps AM, Murphy E. Activation of a novel estrogen receptor, GPER, is cardioprotective in male and female rats. Am J Physiol Heart Circ Physiol 2009; 297:H1806–H1813.
10. Holm A, Hellstrand P, Olde B, et al. The G protein-coupled estrogen receptor 1 (GPER1/GPR30) agonist G-1 regulates vascular smooth muscle cell Ca^{2+} handling. J Vasc Res 2013;50:421–429.
11. Carroll KJ, Esain V, Garnaas MK, et al. Estrogen defines the dorsal-ventral limit of VEGF regulation to specify the location of the hemogenic endothelial niche. Dev Cell 2014;29:437–453.
12. Sander JD, Cade L, Khayter C, et al. Targeted gene disruption in somatic zebrafish cells using engineered TALENs. Nat Biotechnol 2011;29:697.

13. Goessling W, North TE, Loewer S, et al. Genetic interaction of PGE2 and Wnt signaling regulates developmental specification of stem cells and regeneration. Cell 2009;136:1136–1147.
14. Goessling W, North TE, Lord AM, et al. APC mutant zebrafish uncover a changing temporal requirement for wnt signaling in liver development. Dev Biol 2008; 320:161–174.
15. Jayasinghe BS, Volz DC. Aberrant ligand-induced activation of G protein-coupled estrogen receptor 1 (GPER) results in developmental malformations during vertebrate embryogenesis. Toxicol Sci 2012;125:262–273.
16. North TE, Babu IR, Vedder LM, et al. PGE2-regulated wnt signaling and N-acetylcysteine are synergistically hepatoprotective in zebrafish acetaminophen injury. Proc Natl Acad Sci U S A 2010;107:17315–17320.
17. **Cox AG**, **Hwang KL**, Brown KK, et al. Yap reprograms glutamine metabolism to increase nucleotide biosynthesis and enable liver growth. Nat Cell Biol 2016; 18:886–896.
18. Spitsbergen JM, Tsai HW, Reddy A, et al. Neoplasia in zebrafish (Danio rerio) treated with 7,12-dimethylbenz[a] anthracene by two exposure routes at different developmental stages. Toxicol Pathol 2000; 28:705–715.
19. Yuan M, Breitkopf SB, Yang X, et al. A positive/negative ion-switching, targeted mass spectrometry-based metabolomics platform for bodily fluids, cells, and fresh and fixed tissue. Nat Protoc 2012;7:872–881.
20. Sun J, Huang YR, Harrington WR, et al. Antagonists selective for estrogen receptor alpha. Endocrinology 2002;143:941–947.
21. Compton DR, Sheng S, Carlson KE, et al. Pyrazolo[1,5-a] pyrimidines: estrogen receptor ligands possessing estrogen receptor beta antagonist activity. J Med Chem 2004;47:5872–5893.
22. Bologa CG, Revankar CM, Young SM, et al. Virtual and biomolecular screening converge on a selective agonist for GPR30. Nat Chem Biol 2006;2:207–212.
23. Gorelick DA, Halpern ME. Visualization of estrogen receptor transcriptional activation in zebrafish. Endocrinology 2011;152:2690–2703.
24. Dorsam RT, Gutkind JS. G-protein-coupled receptors and cancer. Nat Rev Cancer 2007;7:79–94.
25. Ding Y, Sun X, Huang W, et al. Haploinsufficiency of target of rapamycin attenuates cardiomyopathies in adult zebrafish. Circ Res 2011;109:658–669.
26. Curado S, Anderson RM, Jungblut B, et al. Conditional targeted cell ablation in zebrafish: a new tool for regeneration studies. Dev Dyn 2007;236:1025–1035.
27. Shan J, Schwartz RE, Ross NT, et al. Identification of small molecules for human hepatocyte expansion and iPS differentiation. Nat Chem Biol 2013;9:514–520.
28. Manning BD, Cantley LC. AKT/PKB signaling: navigating downstream. Cell 2007;129:1261–1274.
29. Laplante M, Sabatini DM. mTOR signaling in growth control and disease. Cell 2012;149:274.
30. Evans NJ, Bayliss AL, Reale V, et al. Characterisation of signalling by the endogenous GPER1 (GPR30) receptor in an embryonic mouse hippocampal cell line (mHippoE-18). PLoS One 2016;11:e0152138.
31. Lloyd AC. The regulation of cell size. Cell 2013; 154:1194–1205.
32. **Ben-Sahra I**, **Howell JJ**, Asara JM, et al. Stimulation of de novo pyrimidine synthesis by growth signaling through mTOR and S6K1. Science 2013;339:1323–1328.
33. **Ben-Sahra I**, **Hoxhaj G**, Ricoult SJH, et al. mTORC1 induces purine synthesis through control of the mitochondrial tetrahydrofolate cycle. Science 2016;351:728–733.
34. Baar EL, Carbajal KA, Ong IM, et al. Sex- and tissue-specific changes in mTOR signaling with age in C57BL/6J mice. Aging Cell 2016;15:155.
35. Tsai S-Y, Rodriguez AA, Dastidar SG, et al. Increased 4E-BP1 expression protects against diet-induced obesity and insulin resistance in male mice. Cell Rep 2016;16:1903–1914.
36. Imamura H, Shimada R, Kubota M, et al. Preoperative portal vein embolization: an audit of 84 patients. Hepatology 1999;29:1099–1105.
37. Kawai T, Yokoyama Y, Kawai S, et al. Does estrogen contribute to the hepatic regeneration following portal branch ligation in rats? Am J Physiol Gastrointest Liver Physiol 2007;292:G582–G589.
38. Umeda M, Hiramoto M, Imai T. Partial hepatectomy induces delayed hepatocyte proliferation and normal liver regeneration in ovariectomized mice. Clin Exp Gastroenterol 2015;8:175.
39. Dai G, Bustamante JJ, Myronovych A, et al. Maternal hepatic growth response to pregnancy in the mouse. Exp Biol Med (Maywood) 2011;236:1322.
40. Gershbein LL. Pregnancy and liver regeneration in partially hepatectomized rats. Proc Soc Exp Biol Med 1958;99:716–717.
41. Naugler WE, Sakurai T, Kim S, et al. Gender disparity in liver cancer due to sex differences in MyD88-dependent IL-6 production. Science 2007;317:121–124.
42. Wei T, Chen W, Wen L, et al. G protein-coupled estrogen receptor deficiency accelerates liver tumorigenesis by enhancing inflammation and fibrosis. Cancer Lett 2016; 382:195–202.
43. Taper HS. The effect of estradiol-17-phenylpropionate and estradiol benzoate on N-nitrosomorpholine-induced liver carcinogenesis in ovariectomized female rats. Cancer 1978;42:462–467.
44. Lee CH, Edwards AM. Stimulation of DNA synthesis and c-fos mRNA expression in primary rat hepatocytes by estrogens. Carcinogenesis 2001;22:1473–1481.
45. Chow PKh, Tai B-C, Tan C-K, et al. High-dose tamoxifen in the treatment of inoperable hepatocellular carcinoma: a multicenter randomized controlled trial. Hepatology 2002;36:1221–1226.
46. Barbare J-C, Bouché O, Bonnetain F, et al. Randomized controlled trial of tamoxifen in advanced hepatocellular carcinoma. J Clin Oncol 2005;23:4338–4346.
47. Williams GM, Iatropoulos MJ, Karlsson S. Initiating activity of the anti-estrogen tamoxifen, but not toremifene in rat liver. Carcinogenesis 1997;18:2247–2253.

48. Thomas P, Pang Y, Filardo EJ, et al. Identity of an estrogen membrane receptor coupled to a G protein in human breast cancer cells. Endocrinology 2005;146:624–632.
49. Villanueva A, Chiang DY, Newell P, et al. Pivotal role of mTOR signaling in hepatocellular carcinoma. Gastroenterology 2008;135:1972–1983.
50. Chen J-S, Wang Q, Fu X-H, et al. Involvement of PI3K/PTEN/AKT/mTOR pathway in invasion and metastasis in hepatocellular carcinoma: association with MMP-9. Hepatol Res 2009;39:177–186.
51. Forbes SA, Beare D, Gunasekaran P, et al. COSMIC: exploring the world's knowledge of somatic mutations in human cancer. Nucleic Acids Res 2015;43:D805.
52. Schulze K, Imbeaud S, Letouzé E, et al. Exome sequencing of hepatocellular carcinomas identifies new mutational signatures and potential therapeutic targets. Nat Genet 2015;47:505.

Author names in bold designate shared co-first authorship.

Received October 24, 2018. Accepted January 7, 2019.

Reprint requests
Address requests for reprints to: Wolfram Goessling, MD, PhD, Division of Gastroenterology, Massachusetts General Hospital, 45 Fruit Street, Boston, Massachusetts 02114. e-mail: wolfram_goessling@hms.harvard.edu; fax: 617-525-4751.

Acknowledgments
The authors thank Isaac Oderberg from the Goessling lab for creating the visual abstract, John Asara at the Metabolomics Core at the Beth Israel Deaconess Medical Center for assistance with the metabolomics experiments, and staff of Beth Israel Deaconess zebrafish core facility for fish husbandry.

Author contributions: Saireudee Chaturantabut and Wolfram Goessling conceived the study, designed experiments, and analyzed data. Saireudee Chaturantabut conducted all zebrafish experiments. Arkadi Shwartz performed confocal microscopy and Western blots. Kimberley J. Evason acquired human tissues and performed pathologic analysis of zebrafish and human liver tumors. Andrew G. Cox analyzed metabolomics data. Kyle Labella performed mRNA rescue, xenoestrogens, and long-term anastrozole zebrafish experiments. Arnout G. Schepers and Liliana Mancio Silva performed primary human hepatocyte experiments. Song Yang and Yariv Houvras analyzed RNA sequencing data. Mariana Acuña carried out liver cancer cell line experiments. Shannon Romano, Daniel A. Gorelick, David E. Cohen, Leonard I. Zon, Sangeeta N. Bhatia, and Trista E. North provided overall input. Saireudee Chaturantabut, Trista E. North, and Wolfram Goessling wrote the manuscript. All authors reviewed and edited the manuscript.

Conflicts of interest
The authors disclose the following: Wolfram Goessling is a consultant and Leonard I. Zon is a founder of Camp4 Therapeutics which develops treatments for liver diseases.

Funding
This study is supported by National Institutes of Health 5K08CA172288 (to Kimberley J. Evason), R24OD017870 (to Leonard I. Zon and Wolfram Goessling), R37DK048873, R01DK056626 and R01 DK103046 (to David E. Cohen) and R01DK090311 and R01DK105198 (to Wolfram Goessling), and the Claudia Adams Barr Program in Cancer Research (to Wolfram Goessling). Wolfram Goessling is a Pew Scholar in the Biomedical Sciences.

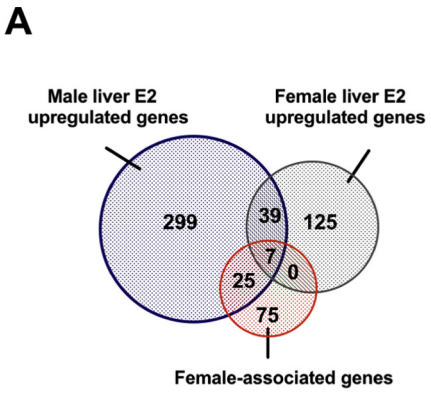

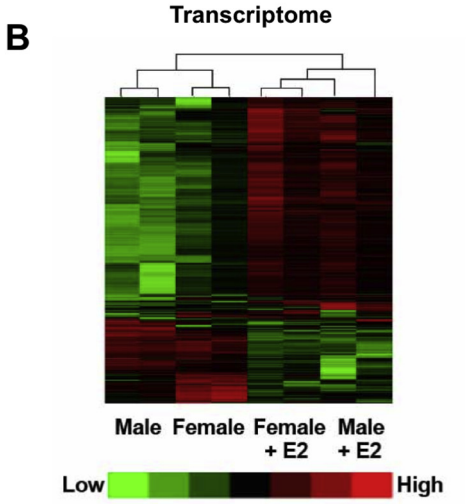

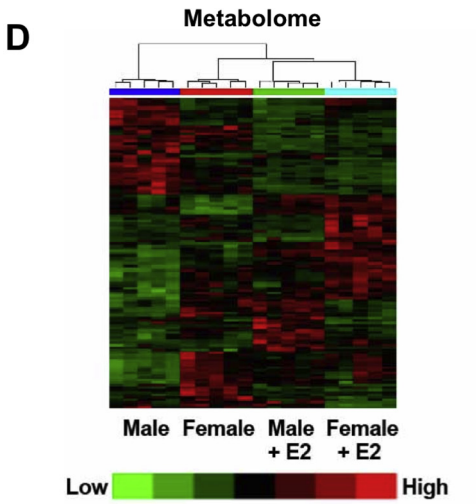

C

Sample	GO Term (Biological Process)	P-Value
Female Liver E2-upregulated genes	Convergent extension involved in gastrulation	2.00E-02
	convergent extension	3.70E-02

E

Sample	Metabolic Pathways	P-Value
Female Liver E2-upregulated metabolites	Ammonia recycling	4.50E-02
	Glutamate metabolism	4.50E-02

Supplementary Figure 1. Estrogen increases liver growth and size. (*A*) Venn diagram showing the intersection of genes differentially expressed in the livers of male vs male + E2, female vs female + E2, and female vs male. (fold change $>$ 10). Values show the numbers of genes up-regulated by E2 in male liver (299 genes), female liver (125 genes), or female-associated liver genes (75 genes). (*B*) Heatmap representing genes significantly enriched upon E2 treatment compared with sex-matched DMSO control of male and female livers (fold change $>$ 10 from DMSO). n = 2 for male, female, male + E2, and female + E2. Scaled expression value is plotted in green-red color scale, with green indicating low expression and red representing high expression. Hierarchical clustering analysis is based on Pearson correlation. (*C*) Transcriptomic analysis showing E2-induced up-regulated genes in female-only livers (fold change $>$ 10 from DMSO). Gene ontology analysis showed up-regulation of genes involved in convergent extension. (*D*) Heatmap representing polar metabolite abundance, as determined by liquid chromatography–tandem mass spectrometry of male and female livers with and without E2. n = 5 for male, female, female + E2, and male + E2. Scaled metabolite abundance values are plotted in green-red color scale, with green indicating low abundance and red representing high abundance. Hierarchical clustering is based on Pearson correlation. (*E*) Polar metabolomics analysis showing significant sex dimorphic differences between DMSO and E2-exposed female-only livers (fold change $\geq$ 2 from DMSO). Metabolic pathway analysis indicated regulation of ammonia and glutamate metabolism. GO, gene ontology.

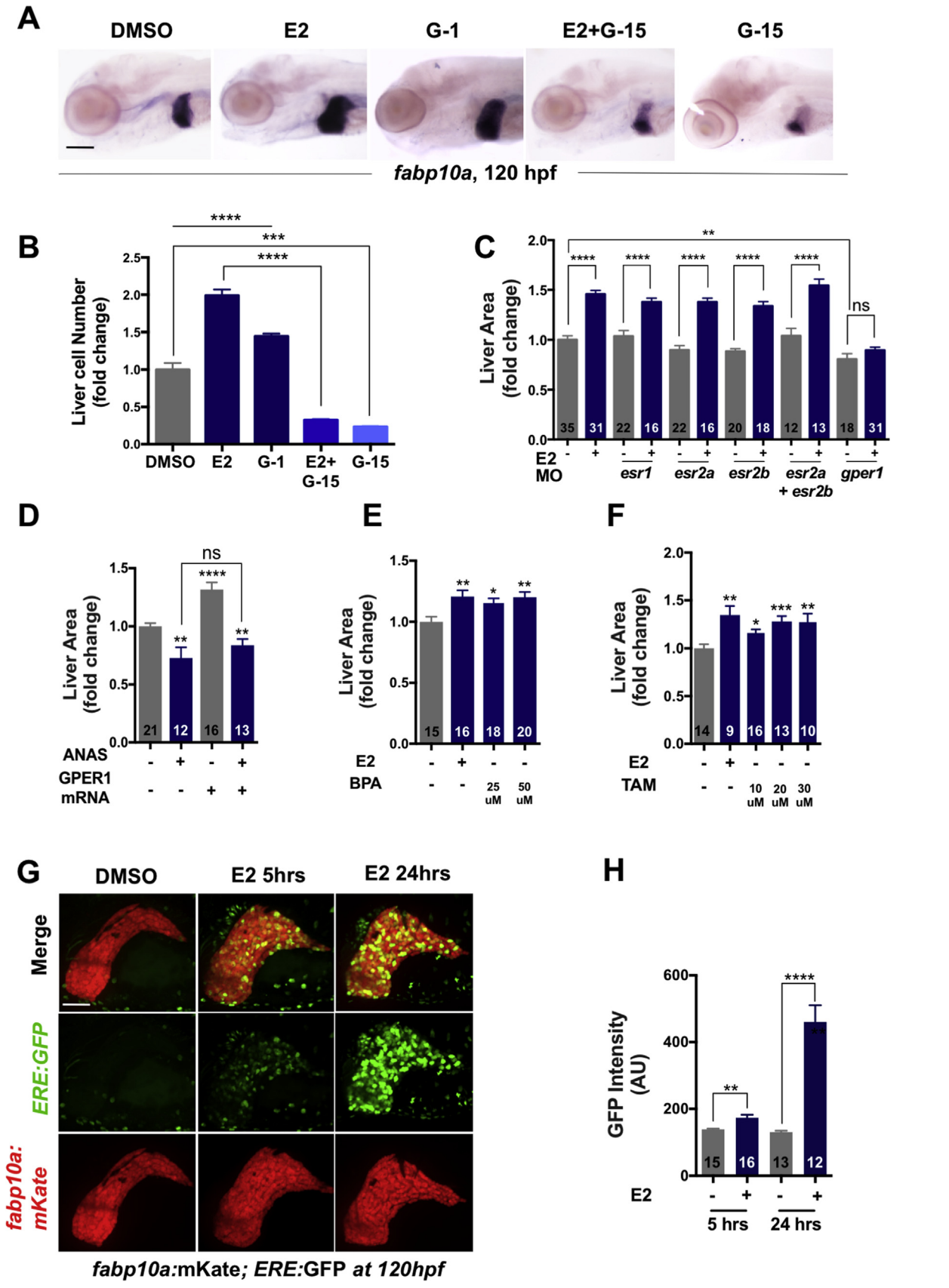
A
DMSO
E2
G-1
E2+G-15
G-15
fabp10a, 120 hpf
B
Liver cell Number (fold change)
DMSO
E2
G-1
E2+ G-15
G-15
C
Liver Area (fold change)
E2
MO
esr1
esr2a
esr2b
esr2a + esr2b
gper1
ns
D
Liver Area (fold change)
ANAS
GPER1 mRNA
ns
E
Liver Area (fold change)
E2
BPA
25 uM
50 uM
F
Liver Area (fold change)
E2
TAM
10 uM
20 uM
30 uM
G
DMSO
E2 5hrs
E2 24hrs
Merge
ERE:GFP
fabp10a: mKate
fabp10a:mKate; ERE:GFP at 120hpf
H
GFP Intensity (AU)
E2
5 hrs
24 hrs

Supplementary Figure 2. GPER1 mediates the estrogenic effects on liver growth. (*A*) Representative images of WT larvae with increased liver size upon E2 or G-1 treatments, decreased liver size upon G-15 treatment, and normalized liver size upon E2 and G-15 cotreatment, as assayed by ISH for *fabp10a* at 120 hpf. Scale bar, 200 μm. (*B*) Quantification of GFP^+ hepatocytes in *fabp10a*:GFP larvae by fluorescence-activated cell sorting (fold change from DMSO). n = 3 independent experiments of 30 pooled larvae, mean ± standard error of the mean. ***$P < .001$, ****$P < .0001$, 2-tailed Student *t* test; ****$P < .0001$, 1-way ANOVA. (*C*) Quantification of liver area as determined by ISH for *fabp10a* (fold change from DMSO). Numbers are as indicated, mean ± standard error of the mean. **$P < .01$, ****$P < .0001$, 2-tailed Student *t* test. (*D*) Quantification of liver area in zebrafish larvae injected with GPER1 mRNA, treated with ANAS (10 μmol/L), or GPER1 mRNA + ANAS (10 μmol/L), as determined by ISH for *fabp10a* (fold change from DMSO). Numbers as indicated, mean ± standard error of the mean. **$P = .06$, ****$P < .0001$, 2-way ANOVA. (*E*) Quantification of liver area in zebrafish larvae treated with DMSO, E2 (10 μmol/L), or bisphenol A (25, 50 μmol/L), as determined by ISH for *fabp10a* (fold change from DMSO). Numbers as indicated, mean ± standard error of the mean. *$P < .05$, **$P < .01$, 2-tailed Student *t* test. (*F*) Quantification of liver area in zebrafish larvae treated with DMSO, E2 (10 μmol/L), or tamoxifen (10, 20, 30 μmol/L), as determined by ISH for *fabp10a* (fold change from DMSO). Number as indicated, mean ± standard error of the mean. *$P < .05$, **$P < .01$, ***$P < .001$, 2-tailed Student *t* test. (*G*) Representative images of Tg(*5xERE:GFP;fabp10a:mKate*) reporter fish exposed to DMSO, 5 hours of E2 and 24 hours of E2 at 120 hpf. Scale bar, 80 μm. (*H*) Quantification GFP intensity of Tg(*5xERE:GFP;fabp10a:mKate*) reporter fish. Numbers as indicated, mean ± standard error of the mean. **$P < .01$, ****$P < .0001$, 2-tailed Student *t* test. ANAS, anastrozole; ns, not significant; AU, arbitrary unit.

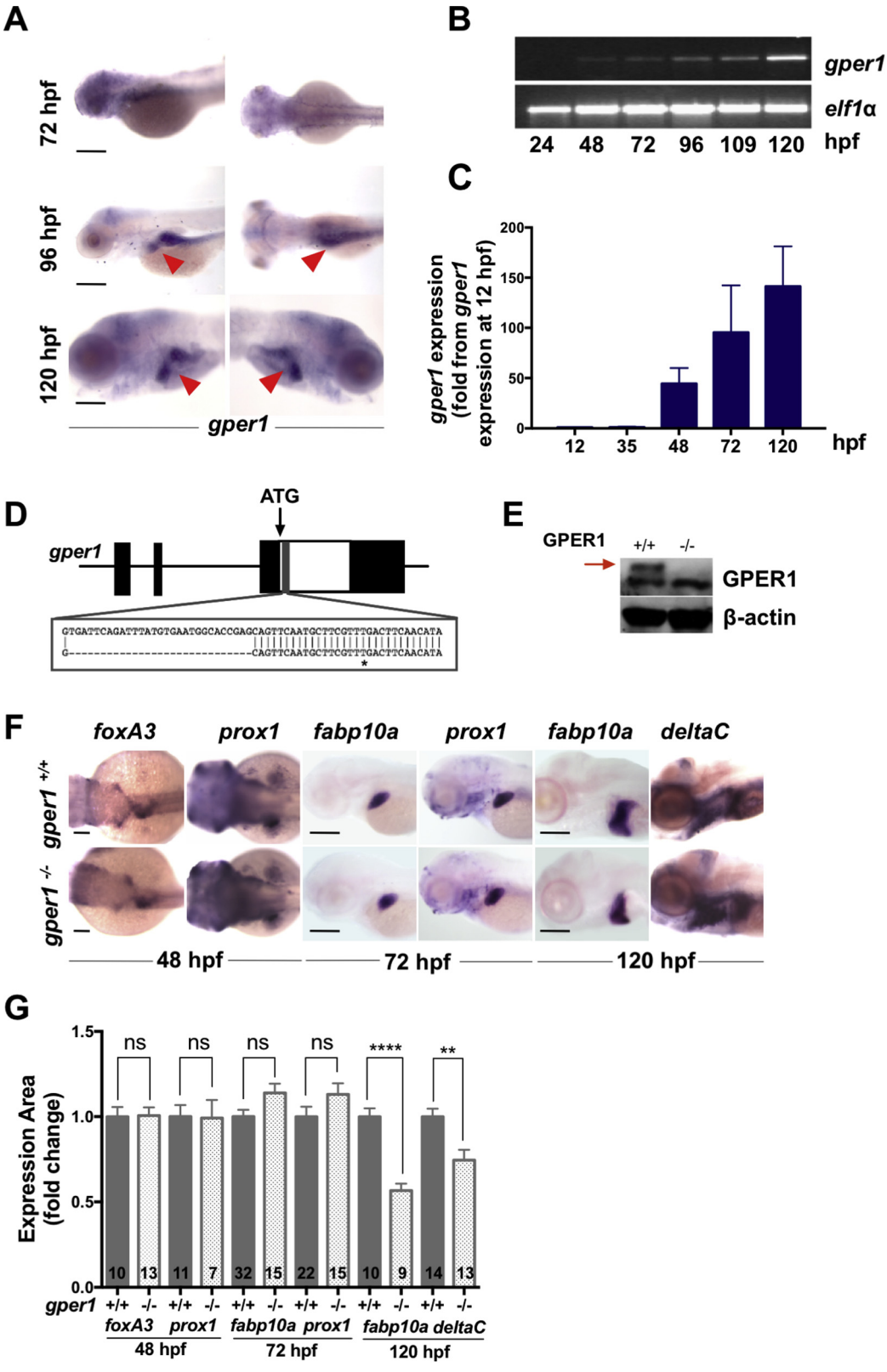
A
72 hpf
96 hpf
120 hpf
gper1
B
gper1
elf1α
24 48 72 96 109 120
hpf
C
gper1 expression (fold from gper1 expression at 12 hpf)
200
150
100
50
0
12 35 48 72 120
hpf
D
ATG
gper1
GTGATTCAGATTTATGTGAATGGCACCGAGCAGTTCAATGCTTCGTTTGACTTCAACATA
G----------CAGTTCAATGCTTCGTTTGACTTCAACATA
*
E
GPER1
+/+ -/-
GPER1
β-actin
F
foxA3 prox1 fabp10a prox1 fabp10a deltaC
gper1 +/+
gper1 -/-
48 hpf
72 hpf
120 hpf
G
Expression Area (fold change)
1.5
1.0
0.5
0.0
ns ns ns ns **** **
10 13 11 7 32 15 22 15 10 9 14 13
gper1 +/+ -/- +/+ -/- +/+ -/- +/+ -/- +/+ -/- +/+ -/-
foxA3 prox1 fabp10a prox1 fabp10a deltaC
48 hpf 72 hpf 120 hpf

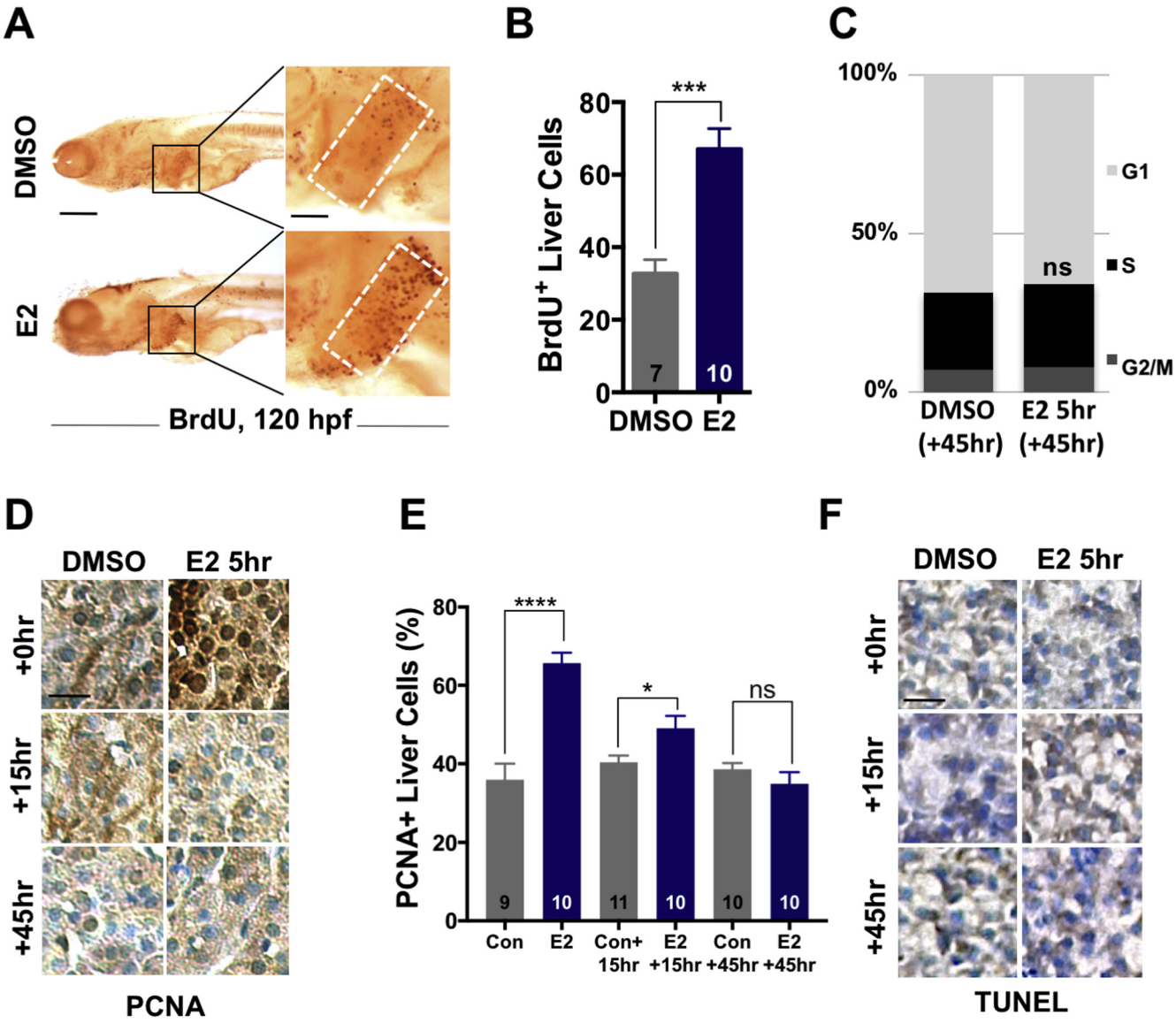

Supplementary Figure 4. Estrogen increases cell proliferation in the liver. (*A, B*) BrdU analysis of whole larvae exposed to DMSO or E2 at 120 hpf. Larvae were pulsed with BrdU and stained for BrdU after fixation. Larvae treated with E2 had more BrdU-positive cells per fixed liver area compared with DMSO-exposed controls. Scale bar, 400 μm; scale bar, (inset) 100 μm. Numbers as indicated, mean ± standard error of the mean. ***$P < .001$, 2-tailed Mann-Whitney test. (*C*) Cell cycle analysis of whole larvae 45 hours after treatment with DMSO or E2 for 5 hours in G1 (*light gray*), S (*black*), or G2/M (*dark gray*) phase. 2-tailed Student *t* test. (*D*) PCNA staining of liver larvae sections. Scale bar, 15 μm. (*E*) Percentage of $PCNA^+$ cells from total hepatocytes in the liver area in larvae at 0, 15, and 45 hours after treatment with DMSO or E2 for 5 hours. Numbers as indicated, mean ± standard error of the mean. *$P < .05$, ****$P < .0001$, 2-tailed Student *t* test. (*F*) TUNEL staining of liver larvae sections. Scale bar, 15 μm. ns, not significant.

Supplementary Figure 3. GPER1 mediates the estrogenic effects on liver growth. (*A*) Lateral and dorsal view of *gper1* expression in larvae at 72, 96, and 120 hpf after ISH for *gper1*. *gper1* is expressed in the liver (*red arrowheads*) starting at 96 hpf. Scale bars, 200 μm. (*B*) Expression of *gper1* transcripts in whole embryo at 24, 48, 72, 96, 109, and 120 hpf, as measured by RT-PCR compared with *elf1*α housekeeping gene control. (*C*) Expression of *gper1* transcripts in whole embryo at 12, 35, 48, 72, and 120 hpf as measured by quantitative RT-PCR (fold change from *gper1* expression at 12 hpf). (*D*) Genomic organization of zebrafish *gper1*. Black boxes represent exons, with antithymocyte globulin site indicated by the arrow. Sequence alignment of $gper1^{+/+}$ siblings and $gper1^{-/-}$ mutant showing TALEN-generated 29-base-pair deletion leading to premature stop codon (*). (*E*) Immunoblot analysis of GPER1 (*red arrow*) and β-actin levels showing loss of GPER1 in $gper1^{-/-}$ mutants compared with $gper1^{+/+}$ siblings. (*F*) Representative images of $gper1^{-/-}$ and $gper1^{+/+}$ larvae ISH for *foxA3* (endoderm) and *prox1* (hepatic progenitor) at 48 hpf, *prox1* and *fabp10a* (hepatocyte) at 72 hpf, and *fabp10a* and *deltaC* (biliary tree) at 120 hpf. Decreased expression levels of *fabp10a* and *deltaC* in $gper1^{-/-}$ compared with $gper1^{+/+}$ were observed only at 120 hpf. Scale bars, 200 μm. (*G*) Quantification of marker expression area in $gper1^{-/-}$ and $gper1^{+/+}$ larvae, as assessed by ISH (fold change from $gper1^{+/+}$). Numbers as indicated, mean ± standard error of the mean. **$P < .01$, ****$P < .0001$, 2-tailed Student *t* test. ns, not significant.

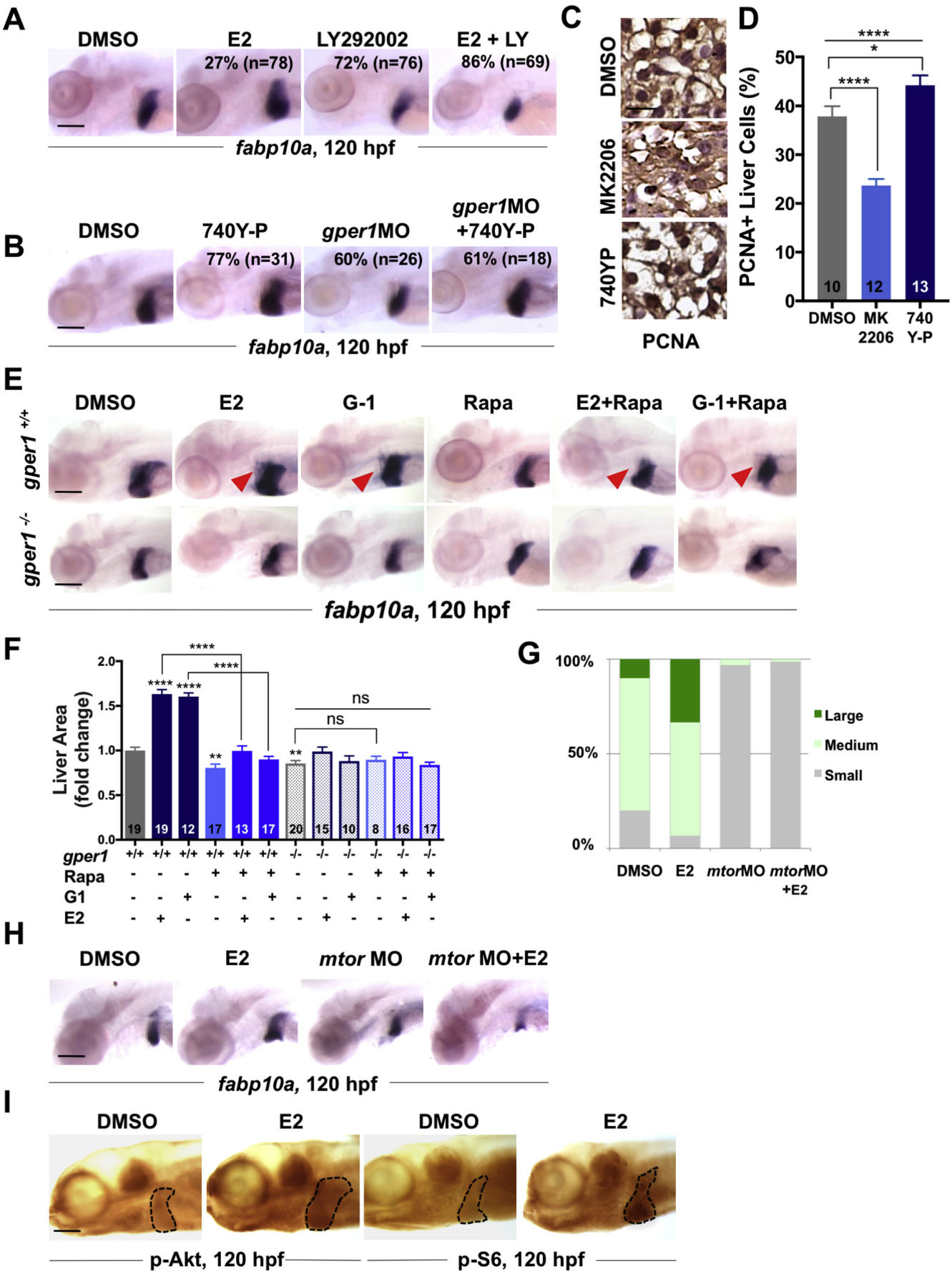
A
DMSO
E2
LY292002
E2 + LY
27% (n=78)
72% (n=76)
86% (n=69)
fabp10a, 120 hpf
B
DMSO
740Y-P
gper1MO
gper1MO +740Y-P
77% (n=31)
60% (n=26)
61% (n=18)
fabp10a, 120 hpf
C
DMSO
MK2206
740YP
PCNA
D
PCNA+ Liver Cells (%)
****
*
****
10
12
13
DMSO
MK 2206
740 Y-P
E
DMSO
E2
G-1
Rapa
E2+Rapa
G-1+Rapa
gper1 +/+
gper1 -/-
fabp10a, 120 hpf
F
Liver Area (fold change)
****
****
****
**
**
ns
ns
19 19 12 17 13 17 20 15 10 8 16 17
gper1 +/+ +/+ +/+ +/+ +/+ +/+ -/- -/- -/- -/- -/- -/-
Rapa - - - + + + - - - + + +
G1 - - + - - + - - + - - +
E2 - + - - + - - + - - + -
G
100%
50%
0%
Large
Medium
Small
DMSO
E2
mtorMO
mtorMO +E2
H
DMSO
E2
mtor MO
mtor MO+E2
fabp10a, 120 hpf
I
DMSO
E2
DMSO
E2
p-Akt, 120 hpf
p-S6, 120 hpf

Supplementary Figure 5. Estrogen signals through GPER1 to activate the PI3K/mTOR pathway to increase liver size. (*A*) Liver size of WT larvae after chemical exposures, as assessed by ISH for *fabp10a* at 120 hpf. E2 exposure increased liver size (21/78 [27%], 21 larvae with phenotype out of 78 total larvae observed), whereas PI3K inhibitor LY292002 decreased liver size (55/76 [72%]). Cotreatment of E2 and LY292002 blocked estrogenic effect on liver size (59/69 [86%]). (*B*) Liver size of WT and *gper1*MO knockdown larvae after chemical exposures at 120 hpf, as assayed by ISH for *fabp10a. gper1* morphants had decreased liver size (15/26 [60%]). Treatment of larvae with the PI3K-activator 740Y-P increased liver size (24/31 [77%]) and rescued small liver phenotype in *gper1* morphants (11/18 [61%]). (*C*) PCNA staining of liver larvae section. Scale bars, 15 μm. (*D*) Percentage of $PCNA^{+}$ cells from total hepatocytes in the liver area. $^{*}P < .05$, $^{****}P < .0001$, 2-tailed Student *t* test. (*E*) Liver size of $gper1^{+/+}$ and $gper1^{-/-}$ larvae ISH for *fabp10a* at 120 hpf after chemical exposures. E2- or G-1–exposed $gper1^{+/+}$ larvae had increased liver size (*red arrowhead*) that can be blocked by coexposure of E2 + rapamycin or G-1 + rapamycin. $gper1^{-/-}$ blocked E2 and G-1 effects on liver size. (*F*) Liver area of $gper1^{+/+}$ and $gper1^{-/-}$ larvae ISH for *fabp10a* at 120 hpf after chemical exposures (fold change from DMSO). Numbers as indicated, mean ± standard error of the mean. $^{**}P = .0323$ vs WT control, $^{****}P < .0001$, 2-way ANOVA. (*G*) Liver size distribution of WT larvae and *mtor* morphants, as assessed by ISH for *fabp10a* at 120 hpf upon exposure to DMSO or E2 as percentage of larvae with large (*dark green*), medium (*light green*), or small (*gray*) livers. (*H*) Liver size of WT and *mtor* morphants as determined by ISH for *lfabp10a* at 120 hpf. (*I*) Whole-mount WT larvae at 120 hpf immunostained for p-Akt and p-S6 upon DMSO or E2 exposure. Liver is outlined in black. All scale bars, 200 μm. ns, not significant.

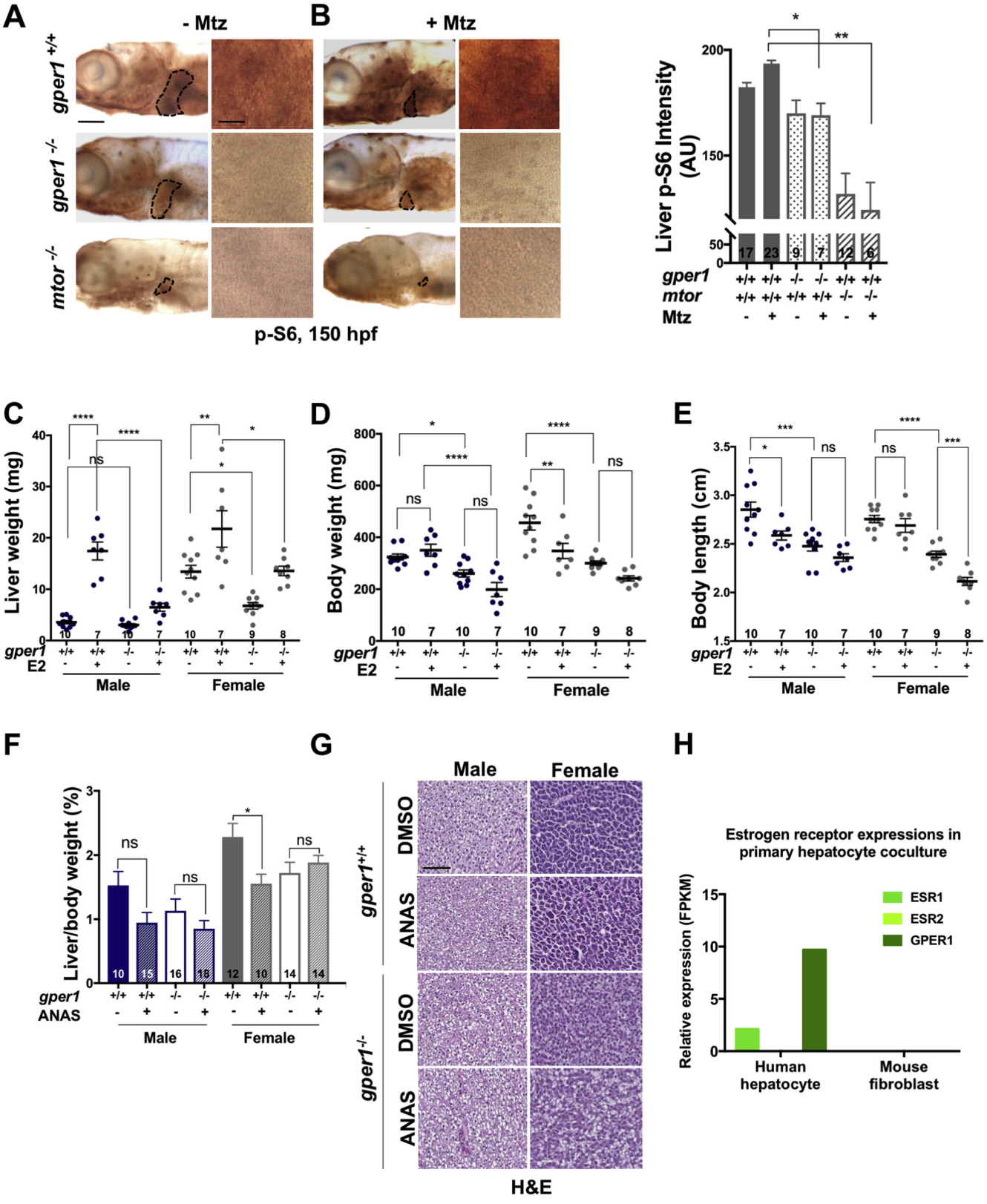
A
- Mtz
B
+ Mtz
gper1 +/+
gper1 -/-
mtor -/-
p-S6, 150 hpf
Liver p-S6 Intensity (AU)
gper1
mtor
Mtz
C
Liver weight (mg)
gper1
E2
Male
Female
D
Body weight (mg)
E
Body length (cm)
F
Liver/body weight (%)
ANAS
G
Male
Female
DMSO
ANAS
H&E
H
Estrogen receptor expressions in primary hepatocyte coculture
Relative expression (FPKM)
ESR1
ESR2
GPER1
Human hepatocyte
Mouse fibroblast

Supplementary Figure 6. GPER1 is essential for regeneration and for male-biased response of estrogen on liver size. (*A*) Whole-mount p-S6 immunostaining showed mTORC1 activation in regenerating WT livers but not in *gper1*$^{-/-}$ or *mtor*$^{-/-}$ livers. Scale bar, 200 μm; insets, 20 μm. (*B*) Quantification of p-S6 intensity from insets in *gper1*$^{+/+}$, *gper1*$^{-/-}$, *mtor*$^{+/-}$, and *mtor*$^{-/-}$ larval livers ± Mtz. *$P = .00568$, **$P < .0001$, 2-way ANOVA; 3 independent experiments, mean ± standard error of the mean, numbers as indicated. (*C*) Liver weight (mg) of *gper1*$^{+/+}$ and *gper1*$^{-/-}$, male and female adult fish treated with DMSO or E2 (10 μmol/L) for 6 weeks. (*D*) Body weight (mg) of *gper1*$^{+/+}$ and *gper1*$^{-/-}$, male and female adult fish treated with DMSO or E2 (10 μmol/L) for 6 weeks. (*E*) Body length (cm) of *gper1*$^{+/+}$ and *gper1*$^{-/-}$, male and female adult fish treated with DMSO or E2 (10 μmol/L) for 6 weeks. (*F*) Liver weight/body weight (%) of *gper1*$^{+/+}$ and *gper1*$^{-/-}$, male and female adult fish treated with DMSO or ANAS (50 μmol/L) for 6 weeks. (*C–F*) *$P < .05$, **$P < .01$, ****$P < .0001$, 2-way ANOVA, sex stratified. (*G*) No significant differences were observed from liver histology of *gper1*$^{+/+}$ and *gper1*$^{-/-}$ male and female adult fish treated with DMSO or ANAS (50 μmol/L) for 6 weeks. (*H*) RNA sequencing data showing relative expression in fragments per kilobase of transcription per million mapped reads (FPKM) of ESR1, ESR2, and GPER1 in human primary hepatocytes and in mouse fibroblast cocultured cells. ANAS, anastrozole; AU, arbitrary unit; ns, not significant.

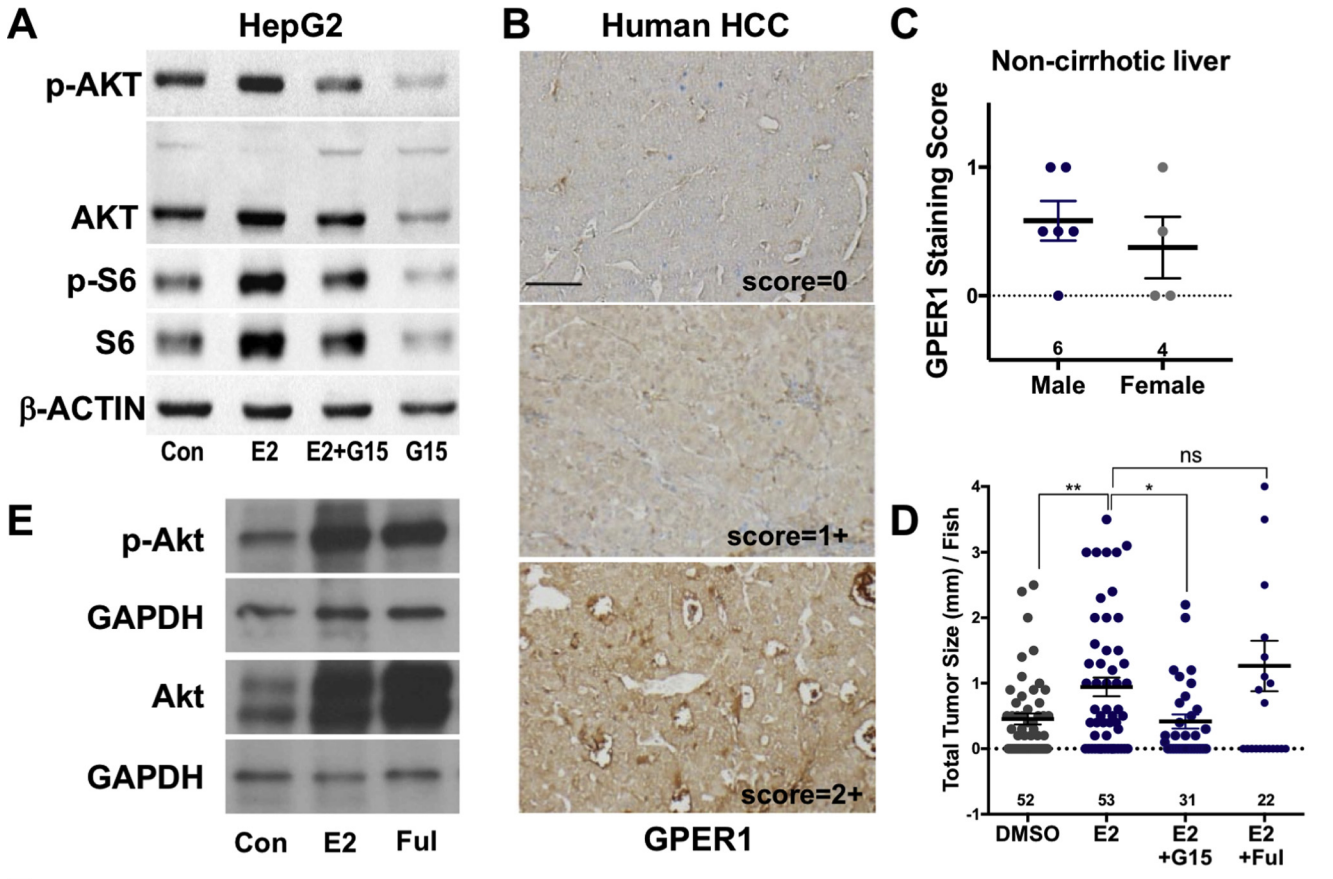
A
HepG2
p-AKT
AKT
p-S6
S6
β-ACTIN
Con
E2
E2+G15
G15
B
Human HCC
score=0
score=1+
score=2+
GPER1
C
Non-cirrhotic liver
GPER1 Staining Score
1
0
6
4
Male
Female
D
ns
**
*
Total Tumor Size (mm) / Fish
4
3
2
1
0
-1
52
53
31
22
DMSO
E2
E2 +G15
E2 +Ful
E
p-Akt
GAPDH
Akt
GAPDH
Con
E2
Ful

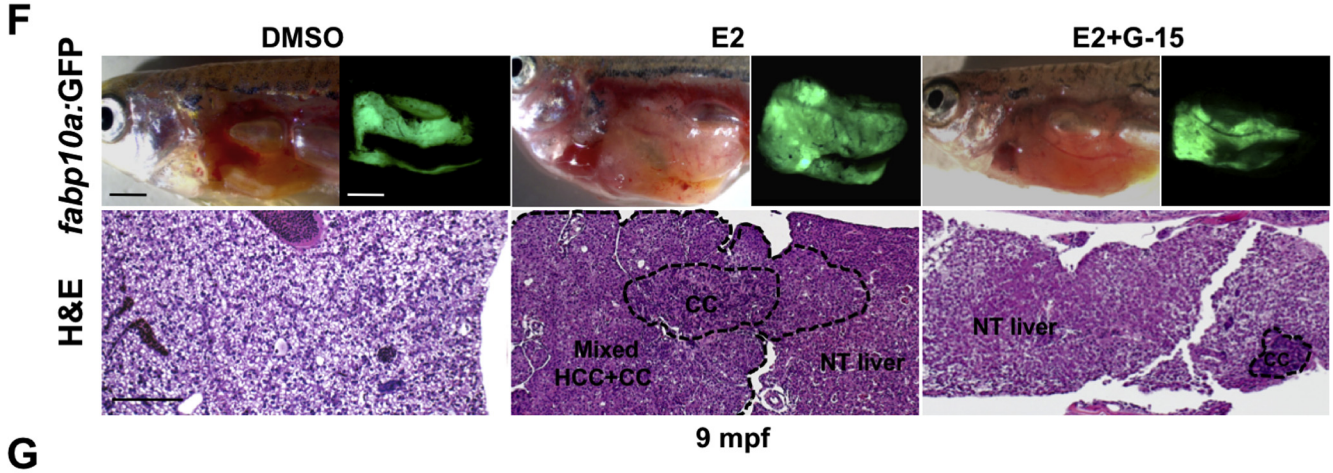
F
DMSO
E2
E2+G-15
fabp10a:GFP
H&E
CC
Mixed HCC+CC
NT liver
NT liver
CC
9 mpf

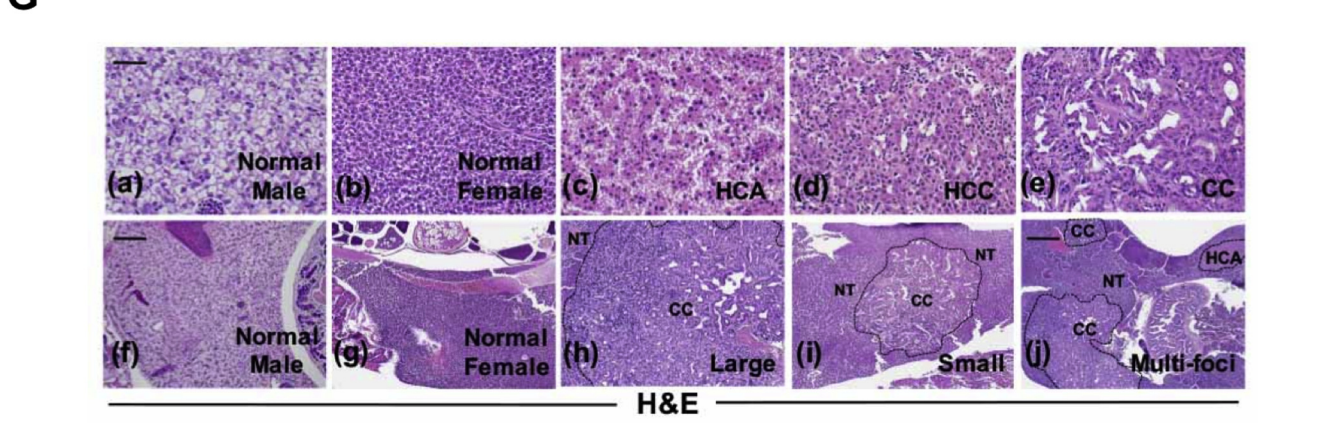
G
(a) Normal Male
(b) Normal Female
(c) HCA
(d) HCC
(e) CC
(f) Normal Male
(g) Normal Female
(h) Large
(i) Small
(j) Multi-foci
NT
CC
HCA
H&E

Supplementary Table 1. Chemicals

Chemical	Concentration	Supplier, catalog number
β-estradiol	10 μmol/L	Tocris (Minneapolis, MN), 2824
MPP dihydrochloride	80 μmol/L	Tocris, 1991
PHTPP	8 μmol/L	Tocris, 2662
G-15	60 μmol/L (embryo) 10 μmol/L (adult)	Tocris, 3678
G-1	8 μmol/L	Tocris, 3577
Anastrozole	10 μmol/L	Tocris, 3388
Fulvestrant, ICI 182,780	10 μmol/L, 15 μmol/L (embryo) 10 μmol/L (adult)	Tocris, 1047
740 Y-P	2 μmol/L	Tocris, 1983
Rapamycin	1 μmol/L	Tocris, 1292
LY294002 HCl	15 μmol/L	Tocris, 1130
NSC 228155	5 μmol/L	Calbiochem (San Diego, CA), 530536
Erlotinib HCl	10 μmol/L	Selleckchem (Munich, Germany), S1023
MK-2206 2HCl	5 μmol/L	Selleckchem, S1078
Metronidazole	10 μmol/L	Sigma, M3761

Supplementary Table 2. Morpholinos

Gene	Sequence (5′→3′)	Type	Amount injected (ng)
esr1	AGGAAGGTTCCTCCAGGGCTTCTCT	ATG	2
esr2a	ACATGGTGAAGGCGGATGAGTTCAG	ATG	2
esr2b	AGCTCATGCTGGAGAACACAAGAGA	ATG	2
gper1	ACATTGGTAGTCTGCTCCTCCATGC	ATG	2
gper1	GCTGCAACACCTGTTATAAGAGAAA	Splice	2
mtor	GGTTTGACACATTACCCTGAGCATG	ATG	2
control	CCTCTTACCTCAGTTACAATTTATA	—	2

Supplementary Table 3. PCR Primers

Gene	Forward primer (5′→3′)	Reverse primer (5′→3′)	LTR (5′→3′)
gper1	TCAAGTTGCCGTCACAATGC	GTCATCCTCTCCCTGTGGTT	—
ef1α	GCGTCATCAAGAGCGTTGAG	TTGGAACGGTGTGATTGAGG	—
mtor	ATAAGAAAAGAAACCACATGTCATACC	CTTACCACTCAGAGAGACCAAAG	CCCTAAGTACTTGTACTTTCACTTG

Supplementary Figure 7. Activation of E2/GPER1 signaling promotes male liver cancer initiation and progression. (*A*) Signaling responses in HepG2 cells to E2 and/or G-15 exposure. (*B*) Representative images of GPER1 staining scoring system. 0, minimal or no staining; 1+, faint/mild staining; 2+, moderate/strong staining. Scale bar, 50 μm. (*C*) Quantification of GPER1 staining scores in noncirrhotic male and female livers. Numbers as indicated, mean ± standard error of the mean. (*D*) Quantification of liver tumor size (mm) per fish in DMBA-exposed WT fish followed by DMSO, E2, E2 + G-15, or E2 + fulvestrant exposure up until 9 months after fertilization. Numbers as indicated, mean ± standard error of the mean. $^{*}P < 0.05$, $^{**}P < 0.01$, 2-tailed Student *t* test. (*E*) Akt signaling responses to E2 and fulvestrant (5 μmol/L) exposure from 110–115 hpf in pooled zebrafish larvae at 120 hpf. (*F*) Tg(*fabp10a*:GFP) fish after chemical treatments and corresponding liver histology. Scale bars (whole animal), 2 mm; scale bars (histology section), 100 μm. (*G*) Histologic features of adult zebrafish liver stained with H&E. Top panel shows zoomed images from (*a*) normal male liver, (*b*) normal female liver, and livers with (*c*) hepatocellular adenoma, (*d*) HCC, and (*e*) cholangiocarcinoma. Scale bar, 25 μm. Bottom panel shows low-magnification images of (*f*) normal male liver, (*g*) normal female liver, and livers with (*h*) large tumor, (*i*) small tumor and (*j*) multifoci tumor. Scale bars in *f–i*, 100 μm; scale bar in *j*, 250 μm. Ful, fulvestrant; GAPDH, glyceraldehyde-3-phosphate dehydrogenase; ns, not significant; NT, nontumor.

Supplementary Table 4. Antibodies

Antibody	Application	Concentration	Supplier, catalog number
anti-PCNA	IHC	1:200	Anaspec (Fremont, CA), AS-55421
anti-pan-cadherin	IF	1:1000	Sigma-Aldrich (St. Louis, MO), C3678
anti-BrdU	Whole-mount IHC	1:500	Sigma-Aldrich, B2531
anti-pEGFR (Tyr1173)	WB	1:1000	MilliporeSigma (Burlington, MA), 05-483
anti-Akt	WB	1:1000	Cell Signaling (Danvers, MA), 9272
anti-pAKT(Ser473)	WB	1:1000	Cell Signaling, 4060
	Whole-mount IHC	1:200	
anti-mTOR	WB	1:1000	Cell Signaling, 2983
anti-S6	WB	1:1000	Cell Signaling, 2217
anti-pS6(Ser240/244)	WB	1:1000	Cell Signaling, 2215
	Whole-mount IHC	1:200	
anti-β-actin	WB	1:5000	Cell Signaling, 4970
anti-rabbit (Alexa Fluor 647)	IF	1:500	Abcam (Cambridge, MA), ab150075
anti-Rabbit IgG-HRP	IHC,WB	1:1000	Santa Cruz (Dallas, TX), sc-2004
anti-GPER1	IHC	1:50	Sigma-Aldrich, HPA027052
anti-HNF4α	IF	1:50	Abcam, ab55223
anti-mouse (Alexa Fluor 488)	IF	1:500	Jackson ImmunoResearch (West Grove, PA)

IF, immunofluorescence; IHC, immunohistochemistry; WB, Western blot.

Supplementary Table 5. Clinical Information for GPER1 Scoring of Noncancer Liver Tissue

Diagnosis	GPER1 score to sort	Reason for biopsy/resection (noncirrhotic liver)	Etiology of cirrhosis	Age and sex
Noncirrhotic liver	1	Liver masses (final diagnosis of hepatocellular adenomas)	—	44F
Noncirrhotic liver	1	Metastatic colorectal cancer	—	43M
Noncirrhotic liver	0.5	Metastatic melanoma	—	76M
Noncirrhotic liver	0.5	Metastatic colorectal cancer	—	33M
Noncirrhotic liver	0.5	Liver mass (final diagnosis of focal nodular hyperplasia)	—	41F
Noncirrhotic liver	0.5	Metastatic colorectal cancer	—	73M
Noncirrhotic liver	0	Autosomal dominant polycystic kidney disease (wedge biopsy of liver taken during bilateral nephrectomy)	—	55M
Noncirrhotic liver	0	Liver masses (final diagnosis of hemangiomas)	—	36F
Noncirrhotic liver	0	Liver mass (final diagnosis of hemangioma)	—	37F
Noncirrhotic liver	1	Liver masses (final diagnosis of hemangiomas)	—	52M
Cirrhosis	0.5		Primary sclerosing cholangitis	27F
Cirrhosis	1	—	Primary sclerosing cholangitis and possible autoimmune hepatitis	24F
Cirrhosis	2	—	Alcohol	39F
Cirrhosis	2	—	Alcohol	41F
Cirrhosis	1.5	—	Alcohol	44M
Cirrhosis	1	—	Non-alcoholic steatohepatitis	34M
Cirrhosis	0.5	—	Primary biliary cirrhosis	45F
Cirrhosis	0.5	—	Non-alcoholic steatohepatitis	52M

F, female; M, male.

Supplementary Table 6. Clinical Information for GPER1 Scoring of Liver Tumor and Adjacent Tissue

Diagnosis	GPER1 score to sort	Paired tissue sample	GPER1 score to sort	Age and sex
Mixed HCC and cholangiocarcinoma	1	ANT (cirrhosis)	2	57F
Mixed HCC and cholangiocarcinoma	1	ANT (cirrhosis)	1.5	58M
Adenocarcinoma	1	ANT (cirrhosis)	1	59M
HCC	1	ANT (cirrhosis)	1.5	76M
HCC	1.5	ANT (cirrhosis)	2	68M
HCC	1	ANT (cirrhosis)	2.5	65M
HCC	1.5	ANT (cirrhosis)	1.5	51M
HCC	2	ANT (cirrhosis)	1.5	62M
HCC	1	ANT (cirrhosis)	2	57F
HCC	2	ANT (cirrhosis)	2	61M
Mixed carcinoma of the liver	1	ANT (cirrhosis)	1.75	64M
HCC	1.75	ANT (cirrhosis)	1.5	73M
HCC	1.5	ANT (cirrhosis)	1.5	57M
HCC	1.75	ANT (cirrhosis)	1.25	59M
HCC	0.5	ANT (cirrhosis)	1	53M
HCC	0	ANT (cirrhosis)	1.5	66M
HCC	0.75	ANT (cirrhosis)	1	60M
HCC	1.25	ANT (cirrhosis)	1	49M
HCC	1.5	ANT (cirrhosis)	1.25	76M
HCC	1.5	ANT (cirrhosis)	1	42M
HCC	1.25	ANT (cirrhosis)	0.75	53M
HCC	0.75	ANT (cirrhosis)	1.25	72M
HCC	1.75	ANT (cirrhosis)	1.5	57M
HCC	2	ANT (cirrhosis)	1	69M
HCC	1.25	ANT (cirrhosis)	0.5	46M
HCC	0	ANT (cirrhosis)	1.25	59M
HCC	1.5	ANT (cirrhosis)	1	58M
HCC	0.75	ANT (cirrhosis)	1	40M
HCC	1.5	ANT (cirrhosis)	1.5	67M
HCC	2	ANT (cirrhosis)	1	82M
HCC	1.5	ANT (cirrhosis)	1.25	71M
HCC	1.5	ANT (cirrhosis)	1.75	56M
HCC	1.5	ANT (cirrhosis)	1.5	57M
HCC	1.75	ANT (cirrhosis)	1.5	74M
HCC	1.25	ANT (cirrhosis)	1	46M
HCC	0.25	ANT (cirrhosis)	1.25	52M
HCC	1.5	ANT (cirrhosis)	1.5	49F
HCC	1.5	ANT (cirrhosis)	1	49M
HCC	1.5	ANT (cirrhosis)	1.25	41M
HCC	1	ANT (cirrhosis)	2.25	45M
HCC	1.75	ANT (cirrhosis)	1.5	65F
HCC	1.5	ANT (cirrhosis)	1.25	69M
HCC	1.5	ANT (cirrhosis)	1.25	45M
HCC	1.75	ANT (cirrhosis)	1.25	57M
HCC	1.5	ANT (cirrhosis)	1.75	62M
HCC	1.75	ANT (cirrhosis)	2	50M
HCC	1.5	ANT (cirrhosis)	1.5	67M
HCC	1.5	ANT (cirrhosis)	1.25	50M
HCC	1.5	ANT (cirrhosis)	2	30M
HCC	1.75	ANT (cirrhosis)	1.5	30M

ANT, adjacent nontumor; F, female; M, male.

Supplementary Table 7. RT-PCR Primers

Gene	Forward primer (5′→3′)	Reverse primer (5′→3′)
gper1	CTCGTGAATAAAGTGTTGCAG	GCAGTCTTGTTTCCTCCAG